DOI: 10.2174/1389203716666150505225744

Send Orders for Reprints to reprints@benthamscience.ae

Current Protein and Peptide Science, 2015, *16*, 735-753

From Conformation to Interaction: Techniques to Explore the Hsp70/ Hsp90 Network

Fernanda A.H. Batista[1], Lisandra M. Gava[2], Gláucia M. S. Pinheiro[3], Carlos H.I. Ramos[3,*] and Júlio C. Borges[1,*]

Júlio C. Borges

[1]*Institute of Chemistry of São Carlos, USP, São Carlos, SP, 13560-970, Brazil;* [2]*Department of Genetics and Evolution, Federal University of São Carlos – UFSCar, São Carlos, SP, 13565-905, Brazil;* [3]*Institute of Chemistry, University of Campinas – UNICAMP, Campinas, SP, P.O. Box 6154, 13083-970, Brazil*

Carlos H.I. Ramos

Abstract: Proteins participate in almost every cell physiological function, and to do so, they need to reach a state that allows its function by folding and/or exposing surfaces of interactions. Spontaneous folding in the cell is in general hindered by its crowded and viscous environment, which favors misfolding and nonspecific and deleterious self-interactions. To overcome this, cells have a system, in which Hsp70 and Hsp90 play a central role to aid protein folding and avoid misfolding. The topics of this review include the biophysical tools used for monitoring protein-ligand and protein-protein interactions and also some important results related to the study of molecular chaperones and heat shock proteins (Hsp), with a focus on the Hsp70/Hsp90 network. The biophysical tools and their use to probe the conformation and interaction of Hsp70 and Hsp90 are briefly reviewed.

Keywords: Analytical ultracentrifugation, Calorimetry, Fluorescence, Molecular chaperones and Hsps, Protein folding, Protein interaction, Thermodynamics.

1. INTRODUCTION

1.1. Protein Folding and Misfolding

The folding of a protein is a critical aspect of cellular physiology, constituting a self-organizing process in which the tertiary structure of a polypeptide chain is dictated by its amino acid sequence [1, 2]. A protein produced in the ribosome achieves its final structure in the cytosol, either spontaneously or with the assistance of specialized proteins known as molecular chaperones (which do not participate in the final structure) or by associating with other partners [2-4]. In a later part of the homeostatic process, proteins are degraded by specific cellular machinery after performing their function.

Protein homeostasis comprises the combination of specific processes that involve synthesis, folding and degradation and are maintained by a complex system known as PQC (protein quality control), wherein molecular chaperones play a pivotal role. Failures in the PQC system can lead to the loss of protein biological function or to the formation of aggregated species, which have been implicated in the aging process and to the development of conformational diseases [2, 4-8].

Thus, the most important functions performed by chaperones are, among others, 1) to assist in the folding of nascent proteins; 2) to prevent aggregation during stressful situations; 3) to assist in addressing proteins for degradation or to organelles; and 4) to rescue proteins from aggregates. According to their molecular mass (*M*), sequence identity and function, chaperones are classified into five major families: Hsp100, Hsp90, Hsp70, Hsp60 and small Hsp (smHsp) (Fig. **1**). Because of their importance in cellular homeostasis maintenance, representatives of each family, with few exceptions, are present in prokaryotes and in almost all cellular compartments of eukaryotes [9]. Hsp70 has a highlighted role in the molecular chaperone network because it functions to receive and handle unfolded/misfolded or partially folded client proteins from other chaperone families, including Hsp90 (reviewed in [3, 10]). The Hsp70 chaperone cooperates with Hsp60/10 transporting client proteins from the ribosome to Hsp60/10 to mediate protein folding [11]. Hsp70 has a dual role in the bi-chaperone system that dissolves protein aggregates. Hsp70 is required in a first step to alter large aggregates by diminishing their size and sending them through the channel of the Hsp100/ClpB molecular chaperone system (second step). In a third step, Hsp70 can receive the remodeled client protein from the Hsp100/ClpB chaperone and act for its proper fate. Therefore, Hsp70 has an upstream and downstream action relative to the Hsp100/ClpB

*Address correspondence to these authors at the Institute of Chemistry of São Carlos, USP, Av. Trabalhador Sancarlense, 400, São Carlos - SP, 13560-970, Brazil; Tel: +5516 33738637; Fax: +5516 33739903;
E-mail: borgesjc@iqsc.usp.br and Institute of Chemistry, University of Campinas – UNICAMP, Campinas - SP, P.O. Box 6154, 13083-970, Brazil; Tel: +5519 35213096; Fax: +5519 35213023;
E-mail: cramos@iqm.unicamp.br

1875-5550/15 $58.00+.00

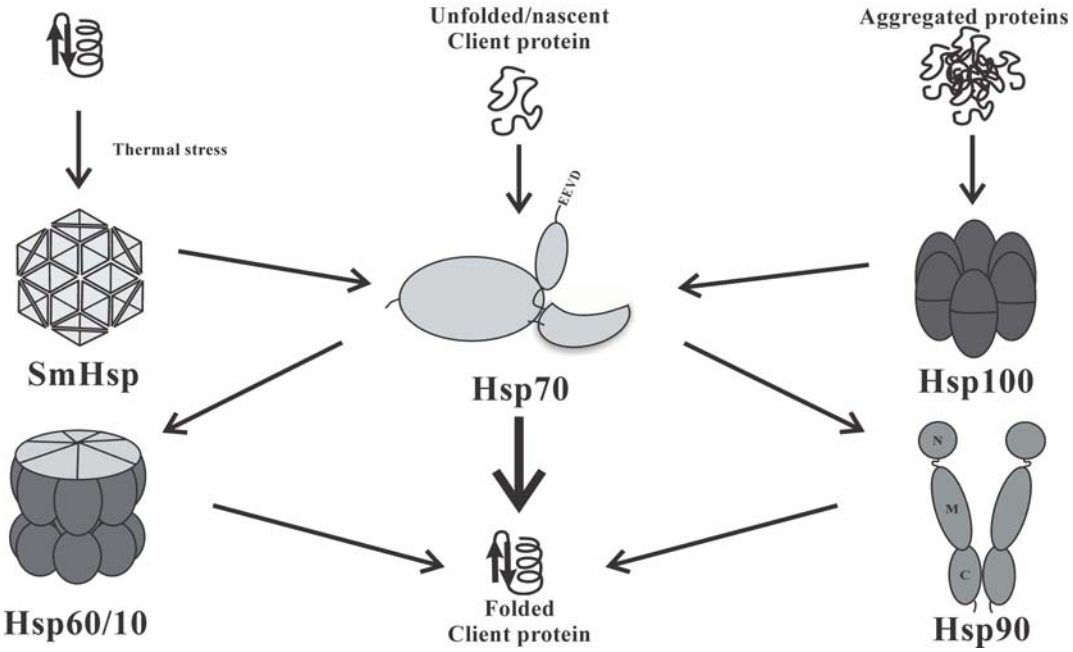

Fig. (1). The pivotal role of the Hsp70 family of proteins, together other chaperone families. Hsp70 receives client proteins directly from the ribosome, and sometimes from other chaperone families, and directs them to Hsp90 and Hsp60/10 for folding. Adapted from [3].

chaperone system [12]. Hsp70 can cooperate with smHsp, which is responsible for reactivating heat-denatured proteins before delivering them to Hsp70 [13]. Chaperones from the Hsp70 and Hsp90 families participate actively and independently in protein homeostasis, but they also function cooperatively in some instances. Indeed, these chaperones act together to form a machinery called foldosome [3, 14, 15]. Apart from the aforementioned roles, molecular chaperones operate through specific physical interactions with the client proteins and are regulated via molecular interactions by small molecules or by their co-chaperones.

1.2. The Hsp70/Hsp90 Network

Hsp70 and Hsp90, as well as some other components of the network, have a common characteristic: they are modular dynamic proteins that can assume different conformations that are under strict control by small ligands and/or by co-chaperones [10, 16-18]. Co-chaperones configure a class of proteins responsible for modulating the activities of the chaperone; for example, they act by inhibiting or promoting ATPase activity and therefore influence the client protein folding. Consequently, understanding co-chaperones is as important as the characterization of the chaperones. Thus, studies on the interaction between Hsp90 and co-chaperones might usefully be considered in the search for Hsp90 inhibitors and their mechanism of inhibition [16, 19].

The Hsp70s are monomeric and modular proteins of approximately 70 kDa formed by two domains. The N-terminal domain contains the NBD (nucleotide binding domain) that is responsible for binding ATP and its hydrolysis, whereas the C-terminal domain is responsible for the interaction with client proteins through the PBD (peptide binding domain) (Fig. **2**). These two domains possess a reciprocal heterotrophic allosterism, which is also regulated by the action of the Hsp70 co-chaperones [10].

The Hsp90s are modular homodimeric proteins (Fig. **3**), where each protomer is 82–96 kDa and can be divided into three distinct and conserved domains [16, 19]. The N-terminal domain (N-domain) is involved in ATP binding and function as an interaction site for some client proteins and co-chaperones. The intermediate or middle domain (M-domain) is involved with client protein interactions and exerts influence on the ATPase activity of the N-domain. The C-terminal domain (C-domain) is responsible for dimerization and also contains interaction sites with client proteins and co-chaperones that possess TPR (Tetratricopeptide Repeat) domains. The interaction with the latter occurs through the specific sequence MEEVD present at the C-termini of Hsp90s, which enables an interaction via a dicarboxylate clamp with the TPR domain [20, 21].

ATP binding and hydrolysis have an essential role for both Hsp70 and Hsp90 chaperone machineries, driving their action mode (Fig. **2** depicts the Hsp70 molecular cycle). In the presence of ATP, Hsp70 possesses an equilibrium of its PBD conformation that is displaced to the open state, which is responsible for its low affinity and fast exchange rates with client proteins. Hydrolysis of ATP by the NBD leads the PBD conformation equilibrium to shift to the closed state [10, 22]. In this conformation, Hsp70 diminishes the exchange rates for client proteins causing an increase in affinity for client proteins. J-proteins (*i.e.*, a class of Hsp70 co-chaperones) interact with the NBD and/or client proteins bound to the PBD and synergistically trigger ATP hydrolysis in the NBD. Therefore, ATPase activity in the NBD is responsible for the transition between the open and closed states of Hsp70 [10]. In the next step of the cycle, the NBD releases ADP and allows ATP re-binding by stimulation of nucleotide exchange factors (NEF), which form an eclectic class of Hsp70 co-chaperones. This action induces conformational changes in the PBD to the open state, which results in the release of the client protein [10]. Alternatively, the

Hsp70-interacting protein (HIP) co-chaperone may act by stabilizing the Hsp70-ADP state, which maintains the Hsp70 bound to the client protein. This complex, which also remains bound to the J protein co-chaperone, can follow a different fate in the cell depending on additional co-chaperone binding to the EEVD motif located in the Hsp70 C-termini end (Fig. **2**). For instance, co-chaperones, such as the Hsp70-Hsp90 organization protein (HOP) or the small glutamine-rich tetratricopeptide repeat-containing protein (SGT), can connect Hsp70-Hsp90 machineries and coordinate the client protein transfer to the latter [23]. If the cell conditions are stressful, the co-chaperone CHIP (carboxyl terminus of the Hsc70-interacting protein) may drive the client protein to degradation through the proteasome machinery. Another possible pathway is to deliver the client protein, for instance, to membrane transportation through the Translocase of Outer Mitochondrial membrane 70 (TOM70) [24].

As previously discussed for Hsp70, Hsp90 also has an ATP hydrolysis driving cycle that requires a series of conformational changes [25, 26]. This cycle is summarized in Fig. (**3**). The ATPase cycle leads, via formation of intermediates, to the closed conformation, in which the N-domains are transiently dimerized and closely associated with the M-domains [25, 26]. Initially, Hsp90 adopts an open "V" conformation in the absence of ATP (**1** in Fig. **3**). The binding of ATP to the N-domain triggers the repositioning of a segment that acts as a lid, leading to a structural rearrangement corresponding to a transient intermediate capable of receiving the client protein (**2** and **2'** in Fig. **3**). At the same time, conformational changes in the Hsp90 closed state, where the N-domains dimerize and further associate with the M-domain (**3** and **3'** in Fig. **3**), lead to ATP hydrolysis (**4** in Fig. **3**). After hydrolysis, the dissociation of the N-domains is followed by the release of both ADP and Pi, which returns Hsp90 to its initial conformation [27]. In addition to the control performed by the ATPase cycle, the Hsp90 conformational cycle is also thermally controlled, which means that all Hsp90 conformations are in an independent thermodynamic equilibrium on the adenosine nucleotide bound state [28]. From this perspective, the ATPase cycle drives the Hsp90 machinery in the clockwise direction [28], as shown in Fig. (**3**).

The widely known mode of interaction between Hsp90 and inhibitory molecules occurs at the N-domain, at the ATP-binding pocket, or through interactions with the C-domain. Compounds able to interact with the N-domain disrupt the closure of Hsp90 and prevent the Hsp90 cycle. The interruption of the cycle is also proposed to explain the inhibition mechanism of ligands, which interact with the C-domain. The inhibition occurs when Hsp90 is in its open conformation, which prevents its dimerization, or via the dimerized C-domain, which does not allow ATP to occupy the N-domain [30]. To our knowledge, only compounds that interact with the N- domain of Hsp90 have currently entered into the clinical testing phase, meaning that compounds that merely share a unique mode of action have reached "after the bench" status. Indeed, despite having been in clinical development since 1999, at this time, there is no Hsp90 drug available on the market either because of problems concerning toxicity, efficacy or pharmaceutical properties [31].

1.3. The Use of Biophysical Tools to Demonstrate the Quality of Recombinant Proteins

In the context of studying protein interactions through *in vitro* approaches, the quality of the proteins to be used in such trials need to be properly assessed. In this regard, protein activity is intrinsically related to protein conformation.

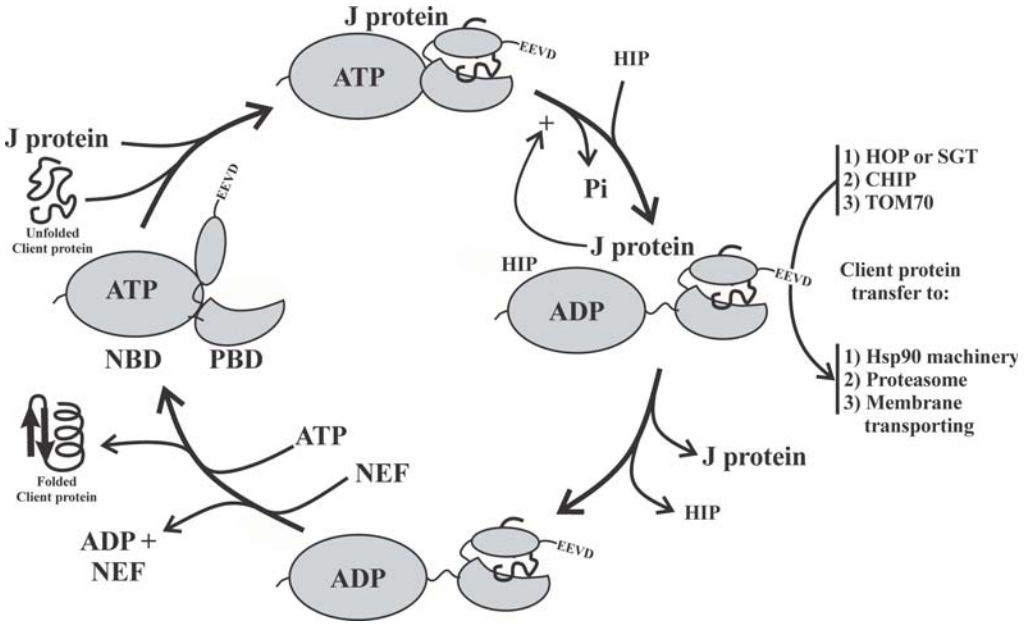

Fig. (2). The Hsp70 molecular cycle and the role of its main co-chaperones. J-protein can deliver the unfolded client protein to the Hsp70 and both synergically stimulate the ATP hydrolysis of the later. After J-protein co-chaperone releases, a NEF induces the ADP output, which allows ATP re-binding and promoting the client protein release. In this point, the Hsp70 is available to other cycle. Alternatively, in the ADP bound state, co-chaperones containing TPR domain, can interact to the complex driving the client protein to different fate (i.e. folding, degradation or translocation) (see text for more details).

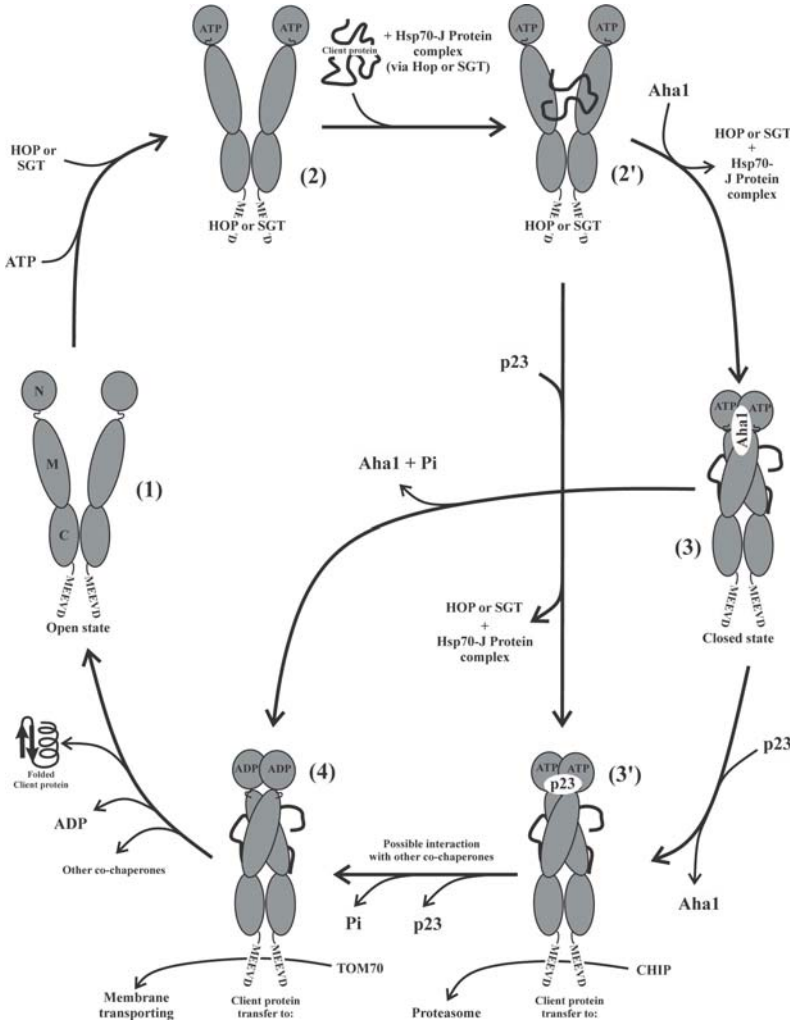

Fig. (3). The Hsp90 molecular cycle and the role of its main co-chaperones. Hsp90 in the open state (**1**) is able to bind to the ATP leading N-domain to a conformation state (**2**) able to receive and interact with the client protein from the *early complex* assisted by the Hop or SGT co-chaperones (**2'**). Conformation changes cause N-domain dimerization leading Hsp90 to the closed state (**3**). In this point, the Hsp90-client protein complex can interact with the Aha1 co-chaperone promoting the Hop or SGT releasing and the stabilization of the complex closed state (**3**). ATP hydrolysis is favored by the closed state and leads to the ADP bound state (**4**). The co-chaperone p23 can disrupt the interaction with Aha1 or, alternatively, can directly bind to the Hsp90-client protein complex (dotted arrow), keeping the Hsp90 in the ATP-bound closed state (**3'**), wherein the ATP hydrolysis is subject to the p23 output. Alternatively, co-chaperones containing TPR domain, can interact to the Hsp90-client protein complex (**3'** or **4**) driving the client protein to different fate (i.e. folding, degradation or translocation). After the ADP release, the folded client protein leaves the complex and follows its proper fate, allowing a new Hsp90 cycle (see text for more details). The Hsp90 ATPase cycle also depends on the interaction with several co-chaperones, including the Hsp70 machinery. Chaperones Hsp70 and Hsp90, as well as some of their co-chaperones, associate in a heterocomplex known as a foldosome [15]. The foldosome assembly occurs sequentially by the association of at least three distinct complexes named *early*, *intermediate* and *late* [23, 29]. The *early* complex is formed when the J protein mediates the interaction of the client protein to Hsp70 (as shown in Fig. **2**). Next, HOP or SGT mediates the physical connection of the Hsp70 *early* complex, which may have HIP bound to it, to the Hsp90/ATP *intermediate* complex, with the subsequent client protein transferred from Hsp70 to the Hsp90 protein. The *late* complex is constructed when Aha1 (activator of the Hsp90 ATPase activity 1) co-chaperones interact with Hsp90, which releases Hsp70, J-protein and SGT/HOP from the *intermediate* complex (**3** in Fig. **3**) [23, 29]. The p23 co-chaperone can also induce the dissociation of the latter proteins from the *intermediate* complex by bypassing Aha1 (**3'** in Fig. **3** – dotted arrow). Therefore, these two Hsp90 co-chaperones regulate the *Hsp90 ATPase* cycle that controls the processing of the client protein and its consequent fate. Aha1 acts by stimulating the Hsp90 ATPase activity and avoiding the participation of p23, whereas p23 acts by displacing Aha1 from Hsp90 and inhibiting its ATPase activity (Fig. **3**). If Hsp90 does not properly fold the client protein or is pharmacologically inhibited, the client protein, mediated by the CHIP co-chaperone, is forwarded to the proteasome machinery (reviewed in [16, 19, 23]).

Moreover, biological activity is indicative of the conformational quality of a protein [32]. Up to July 2011, approximately 100 therapeutic proteins had been approved for clinical use in the European Union and USA, rendering sales that exceeded US$ 100 billion in 2010 [33]. These data corroborate the increase in recombinant protein production, whether for research or pharmaceutical purposes. Furthermore, signify the necessity of controlling the quality of these proteins [34], because safety, efficacy, and quality are of crucial importance for therapeutic drug candidates to gain FDA (Food

and Drug Administration) approval [33]. These safety requirements are intrinsically associated with high-quality proteins with minimal heterogeneity and contamination [33]. Moreover, it is noteworthy that the quality of recombinant proteins also determines its potential use as targets for functional applications or structural analysis [32].

During the recombinant expression of proteins, conformational variants with aberrant biological activities may be generated, leading to the loss of efficacy and safety of the potential medicinal protein. In addition to monitoring the process of protein expression, the purification steps, protein storage and handling must also be monitored. These processes can cause conformational changes that result in inactive or toxic products or generate products with aberrant behaviors [34]. Beyond this, protein structure and conformation will be influenced by experimental conditions such as pH, temperature, and salt concentration, which can favor protein degradation and/or aggregation. Therefore, a stringent control of the conformational state of the protein, as well as of those conditions that can interfere with protein stability, is mandatory during pharmaceutical and research production [35]. These requirements led to the development of guidelines by the International Committee for Harmonization of the US Food and Drug Administration (FDA; guidelines Q6B, Q5E) and the European Medicines Agency (EMA; Comparability of medicinal products containing biotechnology derived proteins), among others [34, 36]. Although the finest means to analyze the conformation of a protein are via biological activity tests, these tools are not always available. To overcome this issue, biophysical methods can be applied to assess the adequacy of a protein's conformation.

The biophysical techniques covered in this review, together with some additional methodologies, represent powerful tools for the characterization and assessments of chaperones. These techniques and methodologies demonstrate the quality of the proteins designed for research, such as those related to the interactions of proteins.

2. PRINCIPLES OF PROTEIN INTERACTIONS

2.1. Specific and Non-Specific Interactions

Protein-ligand or protein-protein interactions are a major event in protein regulation and activity. These relationships are responsible for enzymatic activation and inhibition, conformational changes related to cell signaling, transport and storage of substances, among other important events [37]. In summary, the maintenance of this cellular homeostasis is closely related to the ability of proteins to interact specifically with their target molecules (whether they are small ligands, proteins or other macromolecules). This specificity is related to binding a specific partner and the avoidance of other nonspecific molecules [38]. This 'specificity concept' is essential to understand why proteins are able to manage certain connections correctly, despite a multitude of different interaction possibilities within cellular compartments. Further, it appears that reinforcing interactions are critical for protein homeostasis.

However, the investigation of protein interactions based on specificity is a challenging assignment. All the genome proteins are constructed from the same amino acid blocks, which limits the number of functional protein interfaces that are responsible for conferring the ability of a protein to discern different molecules [39]. According to Johnson and Hummer, the greater the number of proteins in an organism, the greater the occurrence of nonspecific interactions among them [39]. This effect is mitigated when hub proteins that share common and distinct interfaces connect the interaction network. These hub proteins are able to interact with several partners; such multi-specificity is a common feature for proteins involved in signaling and regulation, as is the case of Hsp70 and Hsp90 [38, 40-42]. There are several mechanisms that attempt to explain the apparent promiscuity demonstrated by hub proteins [38]. The first is the existence of interactions through similar complexes that display only slight differences. The second is structural plasticity, *i.e.*, a residue may be important for an interaction with only a subset of partners. Third, the existence of natively unstructured proteins can adopt different structures depending on the complexes with which they are involved. Fourth, post-translational modifications are responsible for the chemical and structural modifications of a protein to promote interactions with different partners. Additionally, molecular compartmentalization and concentration are also a point of control because the protein and the target molecule must be localized near one another and at a specifc concentration to promote their interaction [38].

2.2. Equilibrium Interactions

First, it is imperative to consider that different partners (ligands) can interact with the same protein but with different affinities. In this regard, not only is the 'specificity concept' important but the strength of this binding must also be considered, which is indicated through the association constant (K_A) and the dissociation constant (K_D). We note that the K_D is equal to the inverse of the K_A, which is the ligand concentration required to fill half of the protein binding sites. Because K_D indicates the concentration range in which the dissociation occurs, it is used more extensively than K_A. A wide range of techniques is available for determining the K_D of a protein-protein or protein-ligand ensemble. Methods developed for the study of protein binding can be classified as direct or indirect [43]. Direct methods require the determination of the concentrations of free and bound ligand, being suitable only to those binding reactions that exhibit slow dissociation rates (k_{off}). This approach allows one to measure the ligand fraction before the dissociation of the complex [43, 44]. In contrast, indirect methods provide the extent of binding through the measurement of the fractional saturation and assume that the obtained signal is proportional to the product formation [43, 44]. Considering the different methodologies that are available, there are several techniques that are able to examine protein interactions. Among them, size exclusion chromatography, static and dynamic light scattering, analytical ultracentrifugation, isothermal titration calorimetry and fluorescence spectroscopy are the most commonly used. However, based on the features, assumptions and limitations of each technique, there is no single technique that is suitable to examine all of the possible protein systems. Therefore, this review aims to give a brief description of some of these techniques and explores their use to investigate the conformation and interaction of the Hsp70/Hsp90 network.

3. METHODS FOR STUDYING PROTEIN INTERACTIONS

3.1. Calorimetry

Calorimetry is the thermodynamic field that studies the heat exchange involved in chemical reactions, including that originating from the interaction between two reactants. For biological systems, there are two main calorimetric techniques: Isothermal Titration Calorimetry (ITC) and Differential Scanning Calorimetry (DSC). The functional basis of both techniques is based on the thermal equilibrium (*i.e.*, the "power compensation") between the sample and reference cells [45-47]. A constant current is applied to the reference cell, which activates a feedback circuit that drives a temperature system control in the sample cell. If an exo- or endothermic process occurs in the sample cell, then the device detects the temperature variation and compensates for it, either by cooling or heating the sample cell. This compensation, in watts, is the observed signal that is analyzed by the instrument [46-48]. Therefore, molecular interaction events that give rise to the release or absorption of heat can be detected by a calorimeter.

ITC, due to its versatility and universality, is the main calorimetric technique used for monitoring protein-ligand associations by providing a "thermodynamic signature" of the interaction, which might contribute in elucidating the molecular interaction mechanism [37, 46, 47, 49-52]. The "thermodynamic signature" comprises the K_A, the stoichiometry (n), the interaction enthalpy change (ΔH), the Gibbs free energy variation (ΔG) and the interaction entropy change (ΔS). Based on these thermodynamic parameters, it is possible to differentiate between the protein/ligand interactions that exhibit the same K_A but possess different mechanisms of interaction, depending on their unique entropic and enthalpic contributions [37, 46, 50, 52]. Together with structural information, thermodynamic data obtained by ITC can yield information on the stability of the interaction and assist in identifying key residues directly implicated in the interaction [37, 45-47, 53]. This is one of the reasons that make ITC such a distinguished technique in the development of biopharmaceutical products. Accordingly, ITC has been a widely used tool in drug design [37, 54], especially in helping to identify compounds that show similar affinities, via the enthalpy-entropy compensation phenomenon, but have divergent pharmacokinetic properties [46, 51, 52, 54, 55].

In an ITC experiment, the heat interaction between a titrated ligand (either a protein or other molecule) and a receptor (which is a protein for the purposes of this review), per mol of the ligand, can be analyzed depending on the ligand/receptor molar ratio and it is proportional to the amount of injected ligand [48, 56, 57]. In the early part of the titration, all the added ligand interacts with the free protein in the sample cell. In subsequent titrations, these proteins become saturated and the heat involved in the interaction decreases until it is equal to the heat of the ligand dilution [45]. This process is dependent on [L] and [P], which correspond to the ligand and protein concentrations, respectively; ΔH, n and K_A can be obtained simultaneously in the same experiment (see below). ΔG and ΔS can be calculated from experimental values following the equation:

$$\Delta G = -RT \ln K_A = \Delta H - T\Delta S \qquad \text{Eq. (1)}$$

where R is the universal gas constant and T is the absolute temperature (for reviews, see [37, 45, 47, 50, 57]). ΔH and ΔS reflect global properties of the system and also behave in a compensatory way, such that changes in ΔG are not frequently observed at different temperatures [45, 46, 51, 55]. ΔH is the total heat (ΔH_{total}) absorbed or released by the system through the addition of the ligand and gives information on non-covalent bonds between the ligand and protein such as hydrogen, electrostatic or Van der Waals interactions [45, 46, 50]. Because the measured heat is related to the global effects occurring in the system, ΔH_{total} also depends on the buffer ionization (ΔH_{Buffer}). Therefore, if the experiment is conducted in different buffers, even at the same pH, it is possible to assess the changes in the system ionization [45, 47, 57].

ΔS is related to hydration changes in the system and indicates the degree of water accessibility at the binding site surface. It is also related to the formation of new hydrophobic interactions between the ligand and the protein, which will necessarily result in the exclusion of water. It is important to note that interactions that require the participation of water molecules do not favor entropy; however, they can increase the enthalpy contribution to the process because of the formation of new hydrogen bonds [54]. The reduction of flexibility of the binding site elements such as amino acid side-chains, turns and loops, as well as of the ligand that can become fixed into the binding site, is another source of non-favorable entropy contributions [45, 46, 50].

When ΔH and ΔS are acquired in different temperatures they can provide important information regarding the change in heat capacity (ΔC_p), which is given by the relation:

$$\Delta Cp = \frac{d(\Delta H)}{dT} = \frac{T[d(\Delta S)]}{dT} \qquad \text{Eq. (2)}$$

$\Delta C_p < 0$ is a good indicator of hydrophobic changes caused by the protein-ligand interaction and provides information about the hydration of the system. However, $\Delta C_p > 0$ indicates the formation of electrostatic interactions [17, 47]. In the end, the value of ΔC_p, along with structural high-resolution data, can provide information on the mechanism of interaction and also on the conformational changes caused by the interaction [37, 45-47, 50, 57, 58].

The beauty of the ITC technique is its simplicity that allows obtaining a large amount of thermodynamic and enzyme kinetic parameters from experiments at different temperatures and conditions [45, 59, 60]. The drawback is that the heat observed originates from the general properties of the system [45, 52, 57]. However, it is possible to separate the contributions from different events through a series of experiments [37, 57]. In this way, the ITC technique is useful to determine some of the thermodynamic properties involved in protein-protein and protein-ligand interactions, and the technique is able to relate them to the structural data obtained from other techniques. This technique enables one to 1) compare the K_A determined for similar proteins; 2) evaluate the interaction synergism and the stoichiometry of the system; and 3) obtain information on the stability of the protein-ligand interactions and identify possible conformational

changes caused by the interaction of proteins with their substrates, allosteric ligands, regulatory proteins and potential inhibitors [37, 46].

There are many advantages of the ITC technique compared with the other techniques: 1) heat is a universal probe; 2) ITC generates a constant noise that provides a good signal-to-noise ratio; 3) the detected signal can be used to obtain a time-averaged measurement because it can be measured many seconds after an injection and before the next injection; and 4) the injection is mechanized, which reduces the sampling errors. Considering these advantages and the universality of the probe (*i.e.*, heat) [37, 50], ITC helps to uncover the mechanisms of interaction between ligands and target proteins in four major areas:

1. Protein-protein interaction: few techniques allow studying this type of interaction in solution without the use of extrinsic probes or protein coupling;
2. Protein-ligand interaction: some natural ligands do not absorb light in appropriate electromagnetic regions and require some type of extrinsic probe coupling;
3. Protein-inhibitors interaction: the same characteristics described in the previous item;
4. Protein-peptide interaction: using peptides to understand the mechanism of protein-protein interaction is quite important, but it often requires the peptide to be labeled with an extrinsic probe that allows monitoring complex formation, which increases the peptide production cost and could generate an aberrant result influenced by the presence of the probe.

3.2. Gel Filtration and Light Scattering Techniques

Characterizing the conformation, the oligomerization state of a protein and the stoichiometry of protein-protein interactions are critical in fields such as biochemistry, biophysics and biopharmaceuticals. Thus, different methods can be useful to characterize these protein solution properties. Whereas a modification of the protein structure may possibly distort its conformation and/or interaction, whether by immobilization or through labeling, free-solution and label-free methods are recommended. Analytical ultracentrifugation (AUC) is one of the techniques that can be used to determine solution properties of macromolecules (as addressed in the next section). However, this technique does possess some restrictions, such as requiring extremely pure samples and large quantities of the sample in some trial configurations, in addition to the stability of the sample throughout the experiment, which in some assays can take a few days [61, 62]. The amount of sample required is also a drawback of the ITC method. The use of analytical size-exclusion chromatography (aSEC), also named gel filtration, with online light scattering, eliminates some of the limitations associated with these other techniques.

aSEC has a straightforward methodology and is a rather fast technique. The method separates structures based on molecular size or hydrodynamic volume, more appropriately referred as Stokes' radius (R_s), and is closely correlated to the elution volume of the macromolecule [63]. It is a method commonly applied for estimating *M* of a protein or protein complex [64]. The basic principle of aSEC relies on molecular size separation through a chromatographic column, which is a rigid structure packed with small particles of porous material (*i.e.*, the stationary phase), whereby the sample solution is carried by the solvent (*i.e.*, the mobile phase) permeating the porous particles [63]. The pore sizes of the stationary phase determine the range of sample separation, where large molecules elute first from the column, followed by molecules in decreasing size [65, 66].

The *modus operandi* of aSEC is the partitioning of the molecule between the mobile phase, outside the porous particles of the stationary phase and inside the pores. Based on the equilibrium between the phases, a partition coefficient, K_{av}, can be derived:

$$K_{av} = {V_e - V_0}\Big/{V_t - V_0} \qquad \text{Eq. (3)}$$

where V_e is the elution or retention volume, V_0 is the void or interstitial volume and V_t is the total volume of the column. aSEC is a unique technique in which the partitioning is driven completely by entropic processes; indeed, under suitable experimental conditions, adsorption does not occur during the procedure [67]. K_{av} values range from 0 to 1, which represent a molecule that is totally excluded or non-excluded, respectively. The latter phenomenon indicates that the sample diffuses into all pores and is not adsorbed to the stationary phase [63]. A calibration curve can be generated with the K_{av} versus logarithmic *M* from the standard proteins, after which one can calculate the apparent *M* (M_{app}) for the protein of interest from the acquired K_{av}. The accuracy of the calculated M_{app} depends on the accuracy of the K_{av} determined for the molecule and its correlation with the hydrodynamic properties of the molecule, which constitutes a real challenge with respect to the different symmetries and shapes of biomacromolecules. In fact, it is crucial to note that the molecular shape also has an influence on the elution of the macromolecule through the column, which is a characteristic that, if ignored during aSEC analysis, can generate erroneous information on *M* of a protein or protein-complex.

Nevertheless, it is possible to calibrate aSEC with standard proteins and produce reliable data, but this requires that the calibration be performed using proteins with known R_s values. In fact, the separation occurs as a function of the frictional coefficient *f*, which is the proportionality constant between the particle velocity and frictional resistance [68]. However, because *f* is not an insightful parameter in and of itself, it is normally substituted by R_s. Thus, on the basis of the R_s value obtained by aSEC, a relation between K_{av} versus logarithmic R_s gives estimates on the symmetry/shape, translational diffusion coefficient (*D*) and conformational changes of a protein or protein complex under varied experimental conditions. The relation between *f* and R_s is given by the following equation:

$$f = 6\pi\eta R_S \qquad \text{Eq. (4)}$$

where η is the solution viscosity. From these relations, aSEC can give an R_s relative to R_s from the standards calibration proteins that are common for globular proteins. In addition, R_s can be directly determined from *D*, which is dependent on the size and shape of the molecule:

$$D = \frac{k_B T}{f} = \frac{k_B T}{6\pi\eta R_S} \quad \text{Eq. (5)}$$

where k is Boltzmann's constant. The value for D can be obtained by techniques such dynamic light scattering (DLS) and AUC. In summary, reliable data concerning R_s achieved by the aSEC method must be confirmed and validated by other techniques (*e.g.*, AUC and DLS), which together can afford a wealth of information on the hydrodynamic structure of macromolecules.

Taken together, the conventional aSEC approach introduces several issues in determining the hydrodynamic properties of a protein; one is that the elution volume does not rely simply on the M of the protein but also on its molecular shape. If we consider that common reference standards are globular proteins, this approach can lead to a misinterpretation of the obtained results for any protein. Additionally, there are other features that interfere with aSEC separation processes and disturb the analytical information, such as non-ideal interactions between the protein and the porous particles that constitute the SEC column and also with the mobile phase. Both of these interactions can alter not only the elution time/volume but also the eluting peak shape and recovery of the protein [65, 67]. The necessities of more accurate and reliable information on M and the association/dissociation aspects of molecular interactions have led to techniques that couple aSEC with detectors that are capable of providing these types of data, which is the case for coupling the aSEC separation technique with online light scattering.

Light scattering measurements can produce a set of fundamental information on hydrodynamic properties of macromolecules, such as M, size and D, in addition to interaction properties and dynamics [69]. Depending on the configuration of the light scattering experiments, a measurement may provide different features of these properties. For example, only the size, which is an average over the radius squared, and the weight-average molar mass are obtained in a batch experiment or without separation by aSEC. When a light scattering detector is connected online at the outlet of aSEC columns, a measurement can yield the non-average M and size distribution for the fractioned samples, from which data on the conformation of the macromolecule can be obtained. This ensemble elevates both methods to a new qualitative level of investigation [66].

There are two main light scattering techniques that can be applied to characterize proteins: *static* and *dynamic* light scattering. In the multi-angle static light scattering (SLS or MALS, also termed *elastic*, *Rayleigh* or *classical* light scattering) technique, the time scale of the measurement is long compared to the rapid fluctuations in scattered intensity due to molecular motion. These fluctuations are therefore averaged out, and this technique yields the M, expressed as the root mean square (RMS) radius or radius of gyration and A_2 (*i.e.*, the second virial coefficient) [66, 70].

Dynamic light scattering (also named *quasielastic* light scattering or photon correlation spectroscopy) measures the intensity of the fluctuations of the scattered light. These fluctuations occur because of Brownian motion of the scattered particles and occur over extremely short time intervals. A focused laser beam interacts with the sample and Brownian motion causes scattering of the incident laser light [69]. The result of the measurement is given as a size distribution curve as a function of the intensity of the measured signals. Intensity fluctuations are quantified by an autocorrelation function during periods of time [71]. A slow decay in the autocorrelation function refers to slow fluctuations in intensity, which indicates the presence of large particles, whereas a fast decay indicates small particles. The autocorrelation function is dependent on the refractive index of the medium, the wavelength of the laser and the angle of light scattering [71]. The technique can yield D from the measured decay, which is related to R_s via the Stokes-Einstein equation (Equation 5) [66, 69]. Because D is a function of the size and concentration of the sample, it is possible to analyze the shape of proteins, and it is sometimes possible to obtain insights about their interactions [71]. DLS is a non-destructive, simple and fast technique used to characterize biomacromolecules and their interactions or aggregation, providing dynamic equilibrium properties in solution. DLS presents some practical advantages over MALS because it allows robust measurements in small volumes with free surfaces and because it is relatively unaffected by stray light. Relative to SLS, DLS is not a very sensitive technique and thus it requires higher sample concentrations, which limits the range of binding affinities that can be measured by this technique. For a recent comprehensive treatment of DLS the reader is referred to [61, 69].

The coupling of SEC with a MALS detector consists of an easy, accurate and reliable method, as previously addressed. The basis of calculations performed in SEC-MALS can be assessed by the Rayleigh-Ganz-Debye (RGD) approximation, which is a generalization of light scattering theory that is applicable for particles that are much smaller than the wavelength of the light:

$$R(\theta) = K^* McP(\theta)[1 - 2A_2 McP(\theta)] \quad \text{Eq. (6)}$$

where R is the excess Rayleigh ratio that describes the part of incident light scattered by the macromolecules per unit volume of solution. It is called the *excess* ratio because it accounts for scattered light in excess from the solvent, *i.e.*, for the macromolecule alone. θ is the angle between the incident and scattered light. K^* is the optical constant including the solvent refractive index (n_0), the laser wavelength in vacuum (λ_0) and the specific refractive index increment for the molecule in solution (dn/dc); for a protein or protein complex, the dn/dc value is a constant of approximately 0.187 mL/g (considering no carbohydrates) and describes the change in refractive index of a solution relative to a buffer, due to a mass/volume protein concentration c. $P(\theta)$ is a form function or scattering function and is able to relate the angular variation in scattering intensity to the size of the particle. Finally, A_2 is a thermodynamic term that measures solute-solvent interactions. It is noteworthy that at low protein concentrations, such occurs in aSEC, the A_2 term is negligible; therefore, it is often recognized as a correction factor for concentration effects [66, 69]. In summary, the mathematical approach for SEC-MALS relies on:

$$R(\theta) = K^* McP(\theta); \text{ where } P(\theta) = 1 - \frac{16\pi^2}{3\lambda_0^2}\sin^2(\theta/2)\left\langle R_g^2 \right\rangle + \ldots\ldots \quad \text{Eq. (7; 8)}$$

For further theory and mathematical analysis on light scattering the reader is referred to Philip J. Wyatt [70].

A typical SEC-MALS system uses different detectors in series after the SEC column: the light scattering detector, the absorbance detector and/or the refractive index detector, and a DLS detector can also be connected. More recently, a new method (*i.e.*, composition-gradient (CG)) elevates MALS and DLS to a new level of analysis. This method enables a more accurate and quantitative characterization of protein-protein association/dissociation, with an automated and advanced instrumentation that permits an analysis in a high-throughput style [61, 69, 72].

3.3. Analytical Ultracentrifugation

AUC is an absolute technique, which means that it does not require external standards or probes because it is based on well-founded theories of physical movements (for review, see [73, 74]). Briefly, a particle in a centrifugation tube, which is subjected to a constant angular velocity ω, is forced to the bottom of the tube by the action of the centrifugal force ($F_c = \omega^2 rm$), which depends on the ω, radius (r) and particle mass (m). During its constant migration, the particle also suffers the actions of two resistance forces: 1) the frictional force ($F_f = -fv$), which is proportional to the particle velocity (v) and to f; and 2) the Buoyancy force that "pushes" the particle up when it is immersed in a liquid ($F_{Buy} = -\omega^2 r m_0 = -\omega^2 r m V_{bar}\rho_f$), where m_0 is the fluid weight displaced by the particle. This m_0 is related to the particle m, to the particle partial specific volume (V_{bar}) and to the density of the fluid (ρ_f). Therefore, this force depends on the fluid density and the particle volume. In a situation of constant ω, these forces cancel each other to give zero. The relation can then be solved for v as follows:

$$v = \frac{\omega^2 rm(1 - V_{bar}\rho_f)}{f} \qquad \text{Eq. (9)}$$

Rearranging equation 9, and noting that m depends on the ratio of M and Avogadro's number (N_{av}), the Svedberg equation is obtained:

$$\frac{M(1 - V_{bar}\rho_f)}{N_{Av} f} = \frac{v}{\omega^2 r} \equiv s \qquad \text{Eq. (10)}$$

The term $v/\omega^2 r = s$ is the particle velocity per gravitational acceleration unit, called sedimentation coefficient (s), and is given in 10^{-13} sec or Svedberg (S), named in honor to the AUC "father", Theodore Svedberg. It is worth noting that s increases as a function of M and is inversely proportional to f, indicating that a high M value increases the value of s, whereas an elongated particle shape accounts for reducing the value of s.

Using the above physical principles, two main methods can be applied to AUC: sedimentation velocity (SV) and sedimentation equilibrium (SE) [73, 74]. SV is a method based on hydrodynamic principles, which uses high velocities to sediment the particle while allowing the sedimentation flux to be observed. By using this technique it is possible to obtain information about the particle M and shape directly through s, as well as information about the sample heterogeneity, including K_A in some cases. SE is also based on thermodynamic principles that yield information about M and is independent of particle shape. Additionally in the case of an associative system, it is possible to obtain the interaction K_A and the stoichiometry of the system.

The concentration distribution of the macromolecule in the centrifugal field is observed following the boundary, *i.e.*, the radial concentration gradient profile, which can be obtained by absorption, fluorescence or refraction monitoring. Monitoring the boundary migration profile provides information on the M, shape and the heterogeneity of the particles in solution and is the basis of the SV method [73, 74]. The SV method is subject to the transport effect because the boundary is affected by the gravitational field, as well as by the diffusion arising from the law of mass action. The balance of these two actions can be described by the Lamm equation, [75] which interprets the diffusion interference on the sedimentation process:

$$\frac{d\chi}{dt} = \frac{1}{r}\frac{d}{dr}\left[rD\left(\frac{d\chi}{dr}\right) - s\omega^2 r^2 \chi\right] \qquad \text{Eq. (11)}$$

where χ is the distribution of particle concentration relative to r and the time, and $d\chi/dr$ is the particle concentration gradient in the boundary region.

In a homogeneous system, the boundary shape becomes similar to a sigmoid curve, but in a heterogenic or associative system, the boundary will be represented by a sum of two or more sigmoid curves, depending on how many components are present. Currently, data analyses are performed with software that simulates the Lamm equation (Equation 11) such that the simulated data are fit to the experimental data. In this way, a large data set should be accumulated for the simulation to increase the amount of information obtained [76].

However, if ω is too small, the scattering caused by D is large and can reach the equilibrium between the sedimentation and diffusion forces where there is no transport and $d\chi/dr$ is equal to zero. This occurs because there is no boundary sedimentation flux at equilibrium and the interpretation of the Lamm equation balances the contributions of the terms containing D and s [74]. This is the basis for the SE method. In a system with only one component and without self-association, the particle concentration distribution is an exponential function of the particle buoyant mass ($M(1-V_{bar}\rho)$) and of the square of the radius (r^2). Equation 12 describes the equilibrium between the sedimentation and diffusion forces of a protein of M and V_{bar} in a fluid with density ρ_f. The protein concentration as a function of the radius (c_r), can be obtained by the proportionality enforced by the Beer-Lambert law (in the case of absorbance detection) or another measuring method.

$$C = C_{r_0} e\left[\frac{M(1 - V_{bar}\rho)\omega^2\left(r^2 - r_0^2\right)}{2RT}\right] \qquad \text{Eq. (12)}$$

In this equation, c_{r0} is the protein concentration at a radial distance from the reference position r_0. Because no transport phenomenon interferes in SE experiments, this methodology provides an accurate way to determine the protein M, and

therefore the oligomeric state, and stoichiometry of the protein complexes. SE provides M calculated independently from the determination of D and s, and it is therefore independent of the particle shape [73, 74].

In an ideal associative monomer-n-mer system in equilibrium, the signal recorded in an SE experiment is the sum of the signals generated by the species present in the mixture (monomer and n-mer). In these cases, Equation 12 can be modified to introduce both K_A and n to describe the concentration distribution in the gravitational field:

$$C = C_{mon,r_0} e\left[\frac{M(1-V_{bar}\rho)\omega^2\left(r^2-r_0^{\,2}\right)}{2RT}\right] + K_A\left(C_{mon,r_0}\right)^n e\left[\frac{M(1-V_{bar}\rho)\omega^2\left(r^2-r_0^{\,2}\right)}{2RT}\right] \quad \text{Eq. (13)}$$

Two distinct types of associative systems can be analyzed by AUC: static and dynamic association [77]. In the static association, molecules interact with high K_A and slow k_{off}, allowing the separation of the different components in the experimental time scale. In such cases, SV is the method of choice by allowing the species to also be studied individually from a structural point of view [77]. Furthermore, in the dynamic association systems, the reversibility of the system prevents the separation of species by SV, which causes SE to become the method of choice. However, if the dynamic association system occurs with slow kinetics, problems in reaching the equilibrium state can lead to errors because of the observation time scale [78] and precautions should be taken to ensure that the equilibrium state is reached. The reader should refer to Howlett *et al.* [77] for a presentation of strategies for the SV and SE methods in the study of static and dynamic associative systems.

3.4. Fluorescence

Fluorescence spectroscopy is a biophysical method widely used in different areas of science due to its sensitivity, accuracy, fastness and easiness of use. Experiments are performed in solution, where a bulk average of the features of interest is observed, or in single molecule approaches, which provide more specific information. Fluorescence is a phenomenon in which a molecule (named a fluorophore) emits light from electronically excited states following the absorption of photons [79, 80]. Fluorophores can be a naturally occurring molecule or group (an intrinsic probe) or an introduced fluorophore (an extrinsic probe) that forms a complex with the target molecule [81]. Aromatic amino acids are examples of intrinsic probes, and molecules such as fluorescein, rhodamine and ANS are examples of extrinsic probes. Naturally occurring aromatic amino acids in proteins are considered to be the probe of choice when the local structure of a protein is analyzed through intrinsic fluorescence. Although large changes in protein conformation can modify the fluorescence intensities of tyrosine and phenylalanine, as well as the local mobility of their side chains, they are significantly less useful than tryptophan because of their characteristically low extinction coefficients and quantum yields, coupled with the relative lack of sensitivity to environmental changes [82].

There are two important characteristics of a fluorophore that must be considered in a fluorescence assay: the quantum yield and the lifetime of the excited state of the fluorophore. The quantum yield is a measure of the fluorophore efficiency in emitting the absorbed light, and the fluorescence intensity is proportional to this parameter [80]. The average time that the fluorophore spends in the excited state prior to its return to the ground state is defined as the fluorophore excited state lifetime. This quantity depends on the different radioactive and non-radioactive competitive processes that occur in the fluorophore [79].

Fluorescence is considered to be a local probe, and therefore, the observable fluorescence emission signal obtained in most traditional experiments reports on the environment directly surrounding the analyzed fluorophore [82]. This environmental sensitivity occurs because of competition between the fluorescence emission of the fluorophore with other molecular processes that occur on the time scale of the emission process, which dissipates some of the energy of the excited state [79]. Consequently, the information on the fluorescence emission parameters is limited to the degree of exposure of the fluorophore to the solvent and to the extent of its local mobility [82]. The sensitivity to the changes in the fluorophore environment is one of the reasons that make fluorescence a powerful technique for studying the structure of proteins, including protein-ligand interactions.

There are two types of fluorescence measurements: steady-state and time-resolved. Steady-state measurements are performed with constant illumination and the intensity or emission spectrum is recorded. Because the fluorescence process occurs in nanoseconds, the steady state is reached almost immediately when the sample is exposed to light, making this a widely used technique for analysis [79]. Time-resolved measurements are used for measuring intensity or anisotropy decays. However, because of space limitations, we will focus solely on the steady-state measurements in this review.

Protein interaction assays are designed to target protein conjugates whose intensity changes between the free and bound states [83]. When the intrinsic or extrinsic fluorophore associated with a protein is sensitive to a ligand-binding event, this can be expressed as changes in the absorption or emission spectrum, in the fluorescence decay or in the anisotropy. Therefore, these changes may be used as the observable in the determination of K_A, the binding mode(s), or the rate constant(s) that describe the interaction [84]. Because of the versatility of fluorescence spectroscopy in the study of protein interactions, we will focus primarily on three types of measurements in this review: quenching, anisotropy and differential scanning fluorimetry (also named thermal shift).

Quenching is the name given to any process that leads to a decrease in the fluorescence intensity and can occur through a loss of absorption or a decrease in the quantum yield [79]. Two classes of such processes are of special interest in the study of protein interactions: dynamic and static quenching. Static quenching is related to any process that occurs in the ground state of the fluorophore or immediately following excitation [79]. Dynamic quenching refers to any

process that occurs during the fluorophore excited state lifetime and leads to a change in the fluorescence intensity and lifetime [85]. This type of quenching can involve collisional interactions between the fluorophore and the quencher [79]. The quencher removes a portion of the excitation energy, which leaves less energy for the fluorescence emission [86]. Another dynamic quenching process, which does not require direct contact between the fluorophore and the quencher, is related to Förster Resonance Energy Transfer (FRET) [85, 86]. In this process, the excited fluorophore (a fluorescent donor) transfers a portion of its energy to a fluorophore (a fluorescent acceptor) located near the donor [79, 86]. The overlap between the emission spectrum of the donor and the absorption spectrum of the acceptor and a spatial limit of the distance between both fluorophores are required to achieve a FRET observation. The distance dependence renders the FRET measurements a powerful tool to study intramolecular and intermolecular distances in molecular systems [86].

Upon binding a protein or ligand to a protein molecule, quenching in the observed fluorescence spectrum can be caused by 1) ground-state complex formation between the ligand and the fluorophore(s) in the macromolecule; 2) excited state quenching of the complex; and/or 3) binding-induced structural changes of the protein around the fluorophore [85]. In this way, binding-induced quenching can be static, dynamic, or a combination of both processes [85]. For a simple 1:1 ligand binding, F is the measured fluorescence obtained upon the ligand titration on a fixed starting protein concentration and represents the sum of the free (F_0) and complexed protein (F_p) fluorescence emission intensities. Accordingly, the signal change during a binding experiment is given by [85]:

$$\frac{F_0 - F}{F_0 - F_P} = \frac{[L_T]}{K_D + [L_T]} \qquad \text{Eq. (14)}$$

where $[L_T]$ is the concentration of added ligand. To use Equation 14 effectively, it is mandatory that $[L_T]$ approximate the free ligand concentration $[L_{free}]$, which means that the concentration of the bound ligand remains small relative to the total ligand concentration added in the experiment. Moreover, the inner-filter effect is significant and must also be considered in fluorescence quenching experiments. This effect refers to the light absorbance or dispersion at the excitation or emission wavelength by molecules present in the solution. This effect can be addressed mathematically [85], and the reader is referred to Weert and Stella for equations dealing with ligand depletion [85].

Another approach used to monitor protein-ligand by fluorescence involves anisotropy measurements. In a homogeneous solution, molecules, and hence their fluorophores, are randomly oriented. However, when exposed to the polarized light, fluorophores that have their absorption transition moments oriented in an adequate direction relative to the electric vector of the incident light will be preferentially excited, which results in populating the excited states of the polarized molecules [79]. Consequently, a polarized fluorescence light will be emitted and the extent of this polarization can be described in terms of anisotropy (A) [79]:

$$A = \frac{I\parallel - I\perp}{I\parallel + 2I\perp} \qquad \text{Eq. (15)}$$

where $I\parallel$ and $I\perp$ are the polarized fluorescence emission intensities in the parallel and perpendicular orientations, respectively, relative to the electric vector of the polarized excitation light.

The fundamental anisotropy (A_0) of a fluorophore is obtained when the orientation of the excitation and emission dipoles do not change during the excited state lifetime [80]. However, energy transfer to neighboring molecules and/or motions of the fluorophores can induce a reorientation of the emission dipole during this lifetime, resulting in a depolarization of the system [80]. For biomolecules, the anisotropy is decreased because of rotational diffusion and internal flexibility. In an interaction system, a free fluorophore in solution has a lower A value than when it is bound to a larger molecule, because its rate of rotational diffusion and flexibility will be smaller [79, 80]. If a small fluorophore binds to a protein of a given M, the fluorophore anisotropy will increase with the protein concentration. The measured A, which is obtained from a titration experiment of a protein into a solution containing a small fluorophore, can be related to the fraction of free (A_f) and bound (A_b) fluorophore. By the principle of additivity [87], the measured A is the sum of the fractional anisotropic contributions of the individual species in solution. If the fluorescence is not affected by the binding, the fractional contributions of the free and bound fluorophores will be equivalent to their fractional concentrations [88]. In this way, the molar fraction of the bound fluorophore (f_b) is given by [87]:

$$f_b = \frac{A - A_f}{A_b - A_f} \qquad \text{Eq. (16)}$$

Alternatively, the complex between the protein and a fluorophore probe can be pre-formed and a non-fluorescent compound can be titrated that will displace the fluorophore probe from the complex via competition. In this experiment, A will decrease as a function of the non-fluorescent concentration. In both cases, a curve of A (or f_b) as a function of the protein concentration or competing compound will give the value of K_D. In contrast, if the binding affects the fluorescence intensity of the fluorophore, the fractional intensities of the free and bound species will not be equivalent to their respective molar fractions. The reader is referred to Tetin and Hazlett for the relevant equations that govern situations such as these [88].

Protein conformational stabilization promoted by the binding of a ligand is a phenomenon based on the energetic coupling of the ligand binding and protein melting reactions and is proportional to the ligand binding affinity [89]. This is the principle of several approaches used to measure protein-ligand interactions, including differential scanning fluorimetry (DSF) or thermal shift, which is based on the fact that the fluorescence emission intensity of nonspecific dyes increases with an increase in the hydrophobicity of the environment [90]. In this approach, the dye interacts with hydrophobic

regions that become exposed during the thermally induced unfolding of the protein. In fact, any denaturant can be used, but this technique is usually applied with Peltier controlled plates in which hundreds of samples can be measured simultaneously. In the case of DSF, the dye fluorescence is quenched by water at the beginning of the protein thermal denaturation until the temperature at which the protein quickly unfolds is reached, resulting in the consequent exposure of the hydrophobic core of the protein. At this point, the dye will deliver a higher quantum yield by providing a higher fluorescence emission [90]. Through DSF it is possible to determine the melting temperature (T_m) of the protein, which corresponds to the temperature at the midpoint of the curve transition. The obtained T_m as a function of the ligand concentration can be used to determine the value of K_D [91]. DSF is largely used in ligand screening experiments, where a shift in the T_m obtained in the presence of a ligand relative to that obtained in its absence indicates a positive interaction between the protein and the ligand [90, 91]. Another DSF application aims to optimize the solution phase conditions to stabilize proteins for structural, functional and crystallographic studies [91, 92].

4. BIOPHYSICAL TECHNIQUES AND THE STUDY OF THE HsP70/HsP90 NETWORK

4.1. The Conformation of Hsp70 from Eukaryotes

As discussed in section 2, Hsp70 is involved in promoting the folding of unfolded client proteins and its mechanism of action has been investigated by several research groups. However, several points of this mechanism remain to be elucidated, including its relationship with stress conditions, specific conformational changes, as well as folding process and binding details.

For instance, studies aimed at elucidating the relationship between the structure and function of Hsp70 are important to better understand the mechanism of function of this chaperone. Thus, chaperones from different organisms or organelles have been studied. A gene coding for cytosolic Hsp70 was identified in sugarcane, and the gene was cloned and the recombinant protein purified to validate this candidate [93]. The conformation of the protein was investigated by circular dichroism (CD) spectropolarimetry and tryptophan fluorescence spectroscopy, which showed that the protein was produced in a folded state. Functional experiments evaluating the ability of the protein to function as a foldase, and its ability to interact with J proteins validated the gene as coding a Hsp70 chaperone [93]. Hydrodynamic techniques, mainly AUC and DLS, combined with modeling were used to gain insight on the conformation of the human Hsp70 [94], because only high-resolution structures of the domains of Hsp70 were available.

It is also important to understand whether chaperones could access other oligomeric conformations depending on the environmental conditions. For instance, Hsp70 is prone to oligomerize/aggregate depending on concentration, salt presence and protein storage [95, 96]. Such aggregation propensity is localized in the C-terminal domain, because deletion mutants lacking this domain do not demonstrate aggregation. The aggregation was studied in human Hsp70-1A by pressure denaturation and monitored by fluorescence spectroscopy [95]. The native and pressure denatured forms of Hsp70-1A were then subjected to analysis via aSEC and DLS, which indicated that the protein was a monomer prior to the application of pressure but was translated to oligomers or expanded conformations following pressure denaturation. DLS was used to estimate an R_S value of 3.2 nm for Hsp70. However, the analogous value changed to 5.4 nm following pressure treatment, suggesting that Hsp70-1A had formed oligomers or adopted an expanded conformation. Through atomic force microscopy, it was possible to show that the oligomer formation was not disrupted, even by the addition of ATP or mimetic peptide substrates. Because the oligomer possessed no chaperone activity and demonstrated ATPase activity compatible to that of native Hsp70-1A, it was suggested that the NBD returned to its native folded state following the release of the pressure and that PBD was involved in the chaperone oligomerization [95]. Usually, monomeric proteins are resistant to high pressure; however, Hsp70 was very sensitive to high hydrostatic pressure and formed soluble oligomeric species after the pressure was reduced. This observation raises the possibility that Hsp70 may depend on the activities of other chaperones to prevent the formation of similar oligomers during its folding process [95]. Additionally, even the human mitochondrial Hsp70, or mortalin [97-99], is prone to aggregate [100]. For this reason, the purification of recombinant human mortalin requires a preparative SEC step to separate the aggregates and oligomeric species from the monomeric form, which is necessary to allow its structural and functional characterization.

4.2. Hsp70 Nucleotide Interactions

As mentioned above, the chaperone cycle of Hsp70s is under the control of ATP binding and hydrolysis and the exchange of ADP with ATP (Fig. **2**). Thus, understanding how this occurs is essential to understand the Hsp70 nucleotide modulation. It has been reported previously that the heat-induced unfolding of Hsp70s from *E. coli* [101], which was examined by CD spectropolarimetry at 222 nm, showed two transitions. The first transition is related to the partial unfolding of the NBD, whereas the second transition is related to the complete unfolding of the NBD plus the PBD. The addition of nucleotides (either ATP or ADP) increased the stability of the entire Hsp70s from human and sugarcane, as demonstrated by the increase in T_m in both transitions using CD spectropolarimetry [93, 96]. To understand the changes caused by nucleotides on Hsp70-1A and mortalin, the corresponding chaperones were synthesized and their correct folding was monitored by CD and fluorescence spectroscopies, which were also used to verify ADP and ATP binding [96, 100]. The ADP or ATP binding did not induce a net change in the secondary structure of the protein, but MgATP binding induced a fluorescence quenching on the Hsp70-1A and mortalin emissions. The addition of ADP and ATP (both in the absence and presence of $MgCl_2$) caused an increase in the protein thermal stability, as observed by CD spectroscopy at 222 nm, indicating that the interaction induced conformational changes of the chaperones [96, 100]. ITC was used to compare the thermodynamics of the MgADP and MgATP binding. The results were used to measure K_D and indicated that human Hsp70-1A has a higher affinity for ADP than ATP [96]; however, the opposite effect

was observed for human mortalin [100]. Based on these results, and with a view to achieve additional insight on the behavior of the human Hsp70-1A domains upon nucleotide binding, AUC experiments were performed. These experiments verified that the interaction of ATP induces a significant effect on the conformation of Hsp70-1A [94]. Through the values of *s* and the frictional ratio (f/f_0), it was possible to conclude that nucleotide binding promoted a less elongated Hsp70-1A conformation. To exclude the possibility that these effects were related to Hsp70-1A oligomerization, aSEC, DLS and sedimentation equilibrium AUC measurements were performed, which indicated that Hsp70-1A behaved as a monomer in the absence and presence of both ADP and ATP. These results allow us to conclude that the main conformational change was caused by changes in the relative positions of both the Hsp70-1A domains [94]. ADP and ATP lead to an increase in the stability against pressure induced denaturation of Hsp70-1A [95], in agreement with previous results regarding thermal denaturation [96]. A similar approach was used to investigate the influence of nucleotide binding on Hsp70 from sugarcane (SsHsp70)[93]. By CD spectropolarimetry, the presence of nucleotides demonstrated no effect on the secondary structure of SsHsp70, but the presence of either ATP or ADP increased the thermal stability of SsHsc70. The addition of nucleotides also caused a decrease in the fluorescence intensity emitted by the chaperone. Through functional studies, it was observed that SsHsp70 ATPase activity was stimulated by the presence of J proteins and promoted a refolding of a client protein. An analysis of a cross-linking reaction followed by mass spectrometry suggested that nucleotide-free SsHsp70 was highly dynamic and may fluctuate between different conformations [93]. These results are in agreement with the Hsp70 chaperone cycle presented above.

4.3. Co-Chaperones and its Interaction with Hsp70

CHIP is a TPR containing co-chaperone involved in ubiquitination and the degradation of client proteins and chaperones. It binds to both Hsp70 and Hsp90 and has a major role in the control of degradation/folding. Therefore, it is important to understand how its interactions proceed. In this way, the stoichiometry and K_D of the interaction between human CHIP and the C-terminal peptides of both Hsp70 and Hsp90 were obtained by ITC and aSEC using the full-length chaperones. The combined data from the ITC and aSEC experiments showed that the stoichiometry of interaction is either a dimer of CHIP binding to two Hsp70 monomers or two Hsp90 dimers [102].

HIP is another TPR containing co-chaperone that interacts with the NBD of Hsp70 in the ADP state, which prevents the dissociation of the client protein. A structural analysis of HIP of the protozoa *L. braziliensis* (LbHIP) was performed using a set of biophysics methodology to understand the Hsp70 machinery belonging to this parasite [103]. LbHIP has an R_s value, which is comparable to that found for the human HIP and is higher than would be expected for either a monomeric or dimeric globular protein, as determined by aSEC technique. For all the concentrations tested, sedimentation velocity AUC experiments showed that LbHIP is a highly elongated dimer in solution. Taken together, data from chemical-induced unfolding followed by CD spectropolarimetry and conformational analyses by small angle X-ray scattering (SAXS) showed that LbHIP is a highly flexible dimeric protein that possesses two main domains with different stabilities [103]. The domain structure and elongated shape observed for LbHIP is in agreement with a proposed mechanism in which a dimeric HIP is able to interact with two molecules of Hsp70-ADP bound to a same client protein, increasing the Hsp70 action on this client protein [104].

We also observed that J proteins of human and yeast are modular and flexible dimeric proteins with dimensions long enough to interact with both Hsp70 domains through multiple binding sites [105-108]. J proteins are an eclectic Hsp70 co-chaperone family classified in four types based on domain organization in which the I and II types are the most conserved [108]. Based on the structural and interaction information available on human J proteins from types I and II, a divergent interaction model with Hsp70 was proposed [107]. Additionally, we investigated the stability of the yeast J protein Sis1 and some truncation mutants of its internal subdomains by chemical unfolding followed by CD spectropolarimetry, SV-AUC and SEC-MALS. These experiments allowed us to conclude that the internal subdomain is important to stabilize the Sis1 dimeric structure, which is mediated by the C-terminal region and is thus important for its regulatory action on the Hsp70 molecular cycle [109]. Because J proteins possess different chaperone functions and specific Hsp70 regulatory functions, they can amplify the efficiency of the Hsp70 chaperone by reducing its time spent searching for client proteins [108].

Another interesting example is the human mortalin co-chaperone Hsp70 escort protein 1, or Hep1, which is critical for mortalin solubility and mitochondria biogenesis [110]. Human Hep1 (hHep1) is a 15 kDa protein containing a zinc finger domain. After protein purification by SEC and its protein quality confirmed by SDS-PAGE and CD spectropolarimetry, techniques such as sedimentation velocity AUC and intrinsic fluorescence emission were used to study hHep1. AUC experiments showed that hHep1 has a propensity for oligomerization (in at least four species) that is dependent on the protein concentration, which was confirmed by SAXS experiments [111]. Further, the oligomerization of hHep1 led to changes in the Trp fluorescence emission causing a blue shift, suggesting that Trp in the protein structure is involved in the oligomerization process. Additionally, the role of the zinc ion was critical for protein stability, as indicated by DSC experiments [111].

4.4. Hsp70 and Inhibitor Small Ligands

The function of Hsp70 and DnaK (a bacterial Hsp70) is intrinsically dependent on nucleotide binding and hydrolysis, as described in Fig. (**2**). Therefore, compounds that are able to interfere with the Hsp70 molecular cycle are potential inhibitors of chaperone activity. Two well-known classes of compounds that interact with Hsp70 are molecules able to interact with the ATP binding site and those whose modulation occurs through competition with client proteins. Hsp70 is an allosteric protein [10], and therefore, its interaction with a substrate increases the rate of the ATP hydrolysis and the

interaction with ATP promotes the release of the substrate. In this way, a third class of modulators are recognized as being able to interfere with this allosteric equilibrium [112]. For example, using the bacterial DnaK-DnaJ system, it was found that the flavonoid myricetin diminishes ATP turnover [113]. Using NMR spectroscopy, quenching fluorescence, dynamic simulations and mutant constructions, it was possible to observe that the myricetin-DnaK interaction occurs through a site between the IB and IIB subdomains of DnaK, which is distinct to the site related to ATP binding [113]. Moreover, ATP was able to enhance the interaction affinity between Hsp70 and myricetin [112]. ITC experiments were performed to rule out a potential interaction of myricetin with DnaJ and indicated that the major association involving this ligand occurs with DnaK. FRET assays indicated that myricetin inhibited the binding of DnaJ to DnaK and blocked the co-chaperone activity of DnaJ, even though the interaction occurred at different binding sites. These findings indicated a new "druggable" allosteric site for Hsp70 inhibition [113].

4.5. The Conformation of Hsp90 from Eukaryotes

As discussed for Hsp70, studies aimed at elucidating the relationship between the structure and function of Hsp90 are important to better understand the mechanism of function of this chaperone. The conformation of Hsp90 is conserved among organisms. Nevertheless, some differences exist between Hsp90 from prokaryotes and eukaryotes, such as the presence of a long charged linker between the N- and the M-domains [114]. To determine the importance of this charged linker to the function of Hsp90, the construction of yeast Hsp90 mutants, which lack different residues in this region, were analyzed [114]. The structural stabilities of native and mutant proteins were verified by CD spectropolarimetry, indicating that the mutations had no significant effect on the stability of the protein. Cell viability, chaperone and ATPase activity of the mutants were dependent on the length of the charged linker. A FRET strategy was used to determine the conformational restriction relative to the constructions that lead to cell death. The results indicated that mutants with shorter linkers possessed conformational restriction to achieve the N-Domain dimerized conformation, which is consistent with the rate of ATPase activity. Through surface plasmon resonance and AUC measurements, it was possible to determine that the Hsp90 mutants were not able to interact with either Aha1 or p23 in the same extent as the native protein, suggesting a loss of co-chaperone regulation. Taken together, these data suggest that the charged linker is important to promote protein conformational flexibility and to allow Hsp90 conformational transitions, which ultimately influence the interactions between the co-chaperone and the client protein [114].

Citrus sinensis Hsp90 [115], sugarcane Hsp90 [116] and the *L. braziliensis* Hsp90 (LbHsp90) [18] were analyzed using fluorescence spectroscopy, aSEC, SEC-MALLS, CD spectropolarimetry and AUC. The spectroscopic techniques, *i.e.*, CD and tryptophan fluorescence, were used to evaluate the conformational state of these proteins. CD spectra showed that the chaperones have a large number of alpha helices, and fluorescence showed that the Trps were located in apolar sites, indicating that they were at least partially buried in the structure. The hydrodynamic techniques, *i.e.*, AUC, aSEC and SEC-MALS, were used to show that the Hsp90s were elongated dimers in solution. aSEC was important for showing that LbHsp90 dimers dissociate into monomers with K_D values in the same range as the analogous values for yeast Hsp90 [18]. Information obtained from these analyses has enabled additional studies of these proteins that focus on protein-ligand interactions and assays to investigate prospective inhibitors.

4.6. Hsp90 Nucleotide Interactions

The function of Hsp90 is dependent on its ATPase activity, which is intrinsically related to its conformational state (Fig. **3**). Knowing the importance of the nucleotide interaction to the Hsp90 functionality, it becomes evident that it is also important to analyze the Hsp90-nucleotide interaction. For this reason, several papers addressed the use of different biophysical techniques to examine these interactions. The establishment of the nucleotide affinities toward human Hsp90, along with kinetics measurements, allowed the proposition of the cycle model for human Hsp90 [117]. ATP binding affinities and hydrolysis rates are distinct among different Hsp90s, indicating that chaperones from different organisms are also distinct [23]. For instance, a fluorescence quenching study involving LbHsp90 demonstrated that the affinity of LbHsp90 for ATP is twice that observed to the human Hsp90 [18]. The same authors also used fluorescence quenching to investigate the LbHsp90 interaction with the inhibitor Geldanamycin (GA). The results indicated that LbHsp90 interacts with GA with an affinity similar to that observed for human Hsp90. However, it was observed that the GA affinity for LbHsp90 is lower than for an LbHsp90NM construct, which is also lower than that of the LbHsp90N domain construct. These results indicated that the flexibility of LbHsp90 influences the N-domain interaction with GA, which is particularly important because several drug design approaches are based on the conformation of the N-domain and not that of full-length Hsp90 [18].

The interaction of yeast Hsp90 with adenosine nucleotides and Hsp90 inhibitors was studied by ITC at different temperatures, yielding the ΔCp of the interactions. These experiments were supported by the crystallographic structures of the complexes, which permitted an in-depth analysis of the protein interaction with those ligands [118]. In particular, it was observed that the nucleotide binding site is highly hydrated and that the interaction with adenosine nucleotides is mediated by water molecules, which causes a high entropic cost diminishing the value of K_A. However, the interaction of GA and radicicol inhibitors with the Hsp90 nucleotide binding site led to the release of water molecules, which favor a positive entropic change and increases the values of K_A by 1–2 orders of magnitude in comparison to adenosine nucleotides [118].

4.7. Co-Chaperones and their Interaction with Hsp90

Several proteins that function inside the mitochondria are coded in the nucleus and are thus produced by the ribosomes in the cytoplasm. Hsp90 acts in the transport of nuclear-encoded proteins to the translocation system localized in the membrane of the mitochondria (Fig. **3**). Hsp90 recognizes TOM70, one of the several components of the TOM (*i.e.*,

translocase of the outer membrane) system, to which the unfolded protein is delivered and translocated for eventual folding inside the mitochondria. Most of what is known about the interaction of Hsp90 with TOM70 has come from experiments using the cytosolic fraction of TOM70 [119, 120]. TOM70 is a TPR co-chaperone and this domain is present in the cytosolic fraction of the protein. Biophysical tools were used to confirm the monomeric state of functional human TOM70 [119]. Sedimentation velocity and sedimentation equilibrium AUC were used to demonstrate that TOM70 was primarily a monomer with a small fraction of dimer. In addition, the ITC and SEC-MALS techniques established that the stoichiometry of binding with Hsp90 as being one monomer of TOM70 per dimer of Hsp90 [120]. The data from ITC was also used to compare the thermodynamics of binding between Hsp90 and TOM70 and Hsp90 and HOP. The Hsp90 binding to HOP is relatively strong and enthalpically driven, with an opposite entropic contribution [121]. In contrast, the binding of Hsp90 to TOM70 is relatively weak and is driven both entropically and enthalpically [120]. This investigation suggested that the interaction of TPR proteins with Hsps is more complex and diverse than previously expected.

The interaction mechanism of the Hsp90 co-chaperone Aha1 of *L. braziliensis* (LbAha1) with LbHsp90 was investigated by ITC. Structural studies indicated that LbAha1 is a highly elongated monomer that is composed of two independent domains, which led some to conclude that LbAha1 has dimensions long enough to interact with both the N- and M-domains of LbHsp90 [17]. By measuring ITC injection profiles at different temperatures it was demonstrated that two molecules of LbAha1 interact with one Hsp90 dimer, with a K_D in the micromolar range that is enthalpically driven but with opposing entropic contributions [17]. The latter contribution likely results from the restriction of the flexibility of LbHsp90 because the Aha1 co-chaperone interacts with Hsp90 in the closed state. Additionally, the estimation of ΔCp for the LbAha1-LbHsp90 interaction indicates that the binding occurs primarily via electrostatic interactions, which is similar to the interaction involving the co-crystal of the yeast Hsp90M-Aha1N domains [17].

The p23 co-chaperone inhibits the ATPase activity of Hsp90. Several reports, using multiple techniques, have investigated the basis of its interaction with Hsp90 from different organisms [122-124]. Several trypanosomatides (*i.e.*, organisms with two distinct stages of life) present two p23 co-chaperones, distinguishing them from other organisms, which possess only one p23 orthologue. Two p23 co-chaperones, named Lbp23A and Lbp23B, were identified in the protozoa *L. braziliensis*, and to understand its possible relation to the parasitic adaptation between the insect and mammalian vectors, an exploratory biophysical study was performed [125]. Although both proteins behave as elongated monomers in the solution phase, as demonstrated by aSEC, AUC and SAXS approaches, they possess different resistances to thermal and chemical denaturation, as demonstrated by CD spectropolarimetry, DSC and tryptophan fluorescence spectroscopy [125]. Using ITC, sedimentation equilibrium AUC and fluorescence anisotropy spectroscopy, it was also possible to investigate the interaction of Lbp23A and Lbp23B with LbHsp90 (which established the stoichiometry as one Lbp23 molecule per dimer of LbHsp90) and to analyze the influence of nucleotides on this interaction [125]. Despite the difference in stability, the thermodynamics of interaction obtained by ITC indicates that both Lbp23 proteins interact with LbHsp90 similarly. As reported for LbAha1, the interaction of both Lbp23 with LbHsp90 are enthalpically driven with a large opposite entropic contribution that is likely caused by the restriction of the flexibility of LbHsp90. These results indicate that both Lbp23 co-chaperones interact with the latter in the closed state [125].

4.8. Hsp90 Interaction with Small Ligands

In spite of having been in clinical development since 1999, there is presently no Hsp90 inhibitor available on the market because of concerns regarding toxicity, efficacy or other pharmaceutical properties [31]. Because Hsp90 is a potential target for a myriad of therapeutic strategies, ranging from cancer, neurodegenerative and parasitic diseases [23, 126, 127], it is essential that continuing efforts discover new molecules that modulate the action of Hsp90. This approach must include a search for new modes of interaction, including new strategies for Hsp90 inhibition and co-chaperone modulation [128].

The Hsp90 family is ubiquitously expressed among all organisms, with its homologues present in different cellular compartments. For example, Hsp90α and Hsp90β are present in the cytoplasm, Grp94 is present in the endoplasmic reticulum, and Trap-1 is present in the mitochondria. All of these proteins are paralogues of the human Hsp90 and all play a role in cancer. Characterizing the specificities of the paralogues of Hsp90 inhibitors may result in obtaining selective ligands toward one specific Hsp90, which may decrease possible side effects and toxicity. In this way, after an extensive search for a suitable probe, a fluorescence polarization assay has been shown to be adequate to determine selective interactions between different paralogues, which yields a new strategy for drug development [129]. Another different aspect concerning specificity is related to the differential interaction of the ligand among Hsp90s from distinct organisms. Targeting parasitic Hsp90 is an interesting approach because this chaperone is involved in protein homeostasis, developmental, pathogenesis and adaptive processes [23]. The validation of a potential target needs to consider the specificity of the drug of the parasitic Hsp90 relative to the host Hsp90 to avoid undesirable therapeutics side effects. This aspect was evaluated by the correlation of the *T. brucei* inhibitory growth effect promoted by compounds with biophysical results. A library of known Hsp90 inhibitors was tested by DSF with respect to their ability to interact with different constructions of *T. brucei* Hsp90 and human Hsp90α and Hsp90β, which allowed the identification of potential compounds and its domain binding site [130]. Additionally, the thermodynamic parameters of some promising compounds were obtained by ITC. These results, along with *in vivo* analysis, lead to the selection of compounds that were used in crystallization assays, yielding the mode of interaction and providing valuable structural information to the drug structure-based design [130].

By ITC and DSF measurements, a set of aryl-dihydroxyphenyl-thiadiazole compounds were screened against human Hsp90α. By a detailed thermodynamic analysis, it was possible to identify the contributions from the functional groups, which enabled a rationalization of the efficiency of ligand binding [131]. A pre-determined scaffold containing compounds with antiparasitic activity against *Entamoeba histolytica* and *Giardia lamblia* were tested for their ability to bind to the Hsp90 ATP-binding domain from these organisms through a fluorescent competition assay using bis-ANS as a probe. Based on this study, the *in vivo* efficacy and safety of SNX-5422 (a compound that has already completed the Phase I Trial in patients with hematologic malignancies) was assessed, concluding that Hsp90 is a druggable target in amebiasis and giardiasis therapeutics [132].

Celastrol is a compound isolated from plants with potential anticancer activity [133] that has been reported to interact with Hsp90. An extensive biophysical study of the interaction of this ligand with Hsp90 has been published recently [134]. This study, which used a construction comprising the C-domain of human Hsp90 (C-Hsp90), showed that celastrol binds to the C-domain of Hsp90 and causes oligomerization. In the presence of celastrol, both C-Hsp90 and full-length Hsp90 behaved as large oligomers as measured by DLS and SEC-MALLS. Additionally, the effect was dependent on the concentration of celastrol; in a molar ratio of 1:2 of C-Hsp90:celastrol, the *M* of Hsp90 was that of five dimers, whereas the *M* of Hsp90 was that of seven dimers in a molar ratio of 1:3 [134]. Notably, the presence of celastrol neither affects the binding to the co-chaperone TOM70, as shown by SEC-MALS experiments, nor affects the ability to protect proteins against aggregation, as shown by biochemical studies [134]. However, the stability of Hsp90 is decreased in the presence of celastrol, as shown by both DSC and DSF experiments [134]. A model was proposed in which celastrol causes Hsp90 oligomerization via the C-terminal domain without interfering with its binding to TOM70. Altogether, these results suggest that celastrol interferes with the biological activities of Hsp90 via a specific oligomerization in the C-terminus of Hsp90 that results in destabilization, helping the development of celastrol as a potential compound against tumors.

While most interactions between inhibitors and Hsp90 occur through the chaperone N-terminal, Sansalvamide A-amide (San-A) and its derivative possess a completely different mode of interaction. Through the use of fluorescein-tagged derivatives of San-A and fluorescence anisotropy spectroscopy, it was possible to determine the interaction with the NM domain construction of human and yeast Hsp90 and its preferential binding to the closed conformation, which allosterically modulates the C-terminal client proteins [135].

CONCLUSION

Protein-ligand or protein-protein interactions are a remarkable event in protein function and are critical for cellular homeostasis. Specifically, for the Hsp70 and Hsp90 chaperone families, these interactions are significant to their molecular mechanism, such as driving their chaperone cycles and regulating the fate of client proteins, which also depend on the actions of their corresponding co-chaperones. Additionally, these molecular chaperones undergo a fairly complex regulation via protein-protein and/or protein-ligand interactions, such as their weak ATPase activity that regulates the bound adenosine nucleotide, which exerts another level of control and determines preferential binding among different co-chaperones and the binding or release of client proteins. The fact that both Hsp70 and Hsp90 chaperones are deeply involved within the process of cellular homeostasis makes them promising targets for pharmacotherapy. Therefore, the identification and validation of a good inhibitor for these chaperones depends on the determination of interaction parameters such as selectivity, affinity and stoichiometry; protein structure and dynamics may influence these parameters, either directly or indirectly. Because there is no single technique suitable for analyzing all different types of interactions, different biophysical tools can be used alone or in combination to monitor all facets of the interaction processes. Knowledge of the oligomeric state is also very important to understand the mechanism of the protein action to address, for example, Hsp90 as a dimer may interact with different co-chaperones with different stoichiometries. Therefore, both are meaningful information for understanding the interaction mechanism and the co-chaperone function. Furthermore, the use of structural information, either at high or at low resolution, and biophysical data has been shown to be useful to further our understanding of protein-protein interactions. In summary, we presented distinct biophysical techniques aimed to study and scrutinize the complex interactions occurring in the Hsp70 and Hsp90 systems. The results of such techniques clarify some key points in the mechanisms of action of these systems that can be used as specific points for pharmacological control.

CONFLICT OF INTEREST

The authors confirm that this article content has no conflict of interest.

ACKNOWLEDGEMENTS

CHIR and JCB are CNPq Research Fellows and thank FAPESP, CAPES and CNPq for financial support.

REFERENCES

[1] Stravopodis, D.J.; Margaritis, L.H.; Voutsinas, G.E. Drug-mediated targeted disruption of multiple protein activities through functional inhibition of the Hsp90 chaperone complex. *Curr. Med. Chem.,* **2007**, *14*(29), 3122-3138.

[2] Ramos, C.H.; Ferreira, S.T. Protein folding, misfolding and aggregation: evolving concepts and conformational diseases. *Protein Pept. Lett.,* **2005**, *12*(3), 213-222.

[3] Borges, J.C.; Ramos, C.H. Protein folding assisted by chaperones. *Protein Pept. Lett.,* **2005**, *12*(3), 257-261.

[4] Tiroli-Cepeda, A.O.; Ramos, C.H. An overview of the role of molecular chaperones in protein homeostasis. *Protein Pept. Lett.,* **2011**, *18*(2), 101-109.

[5] Luheshi, L.M.; Crowther, D.C.; Dobson, C.M. Protein misfolding and disease: from the test tube to the organism. *Curr. Opin. Chem. Biol.,* **2008**, *12*(1), 25-31.

[6] Morimoto, R.I. Proteotoxic stress and inducible chaperone networks in neurodegenerative disease and aging. *Genes Dev.,* **2008**, *22*(11), 1427-1438.

[7] Kikis, E.A.; Gidalevitz, T.; Morimoto, R.I. Protein homeostasis in models of aging and age-related conformational disease. *Adv. Exp. Med. Biol.,* **2010**, *694*, 138-159.

[8] Anderson, J.F.; Siller, E.; Barral, J.M. Disorders of protein biogenesis and stability. *Protein Pept. Lett.,* **2011**, *18*(2), 110-121.

[9] Gupta, S.C.; Sharma, A.; Mishra, M.; Mishra, R.K.; Chowdhuri, D.K. Heat shock proteins in toxicology: how close and how far? *Life Sci.,* **2010**, *86*(11-12), 377-384.

[10] da Silva, K.P.; Borges, J.C. The molecular chaperone Hsp70 family members function by a bidirectional heterotrophic allosteric mechanism. *Protein Pept. Lett.,* **2011**, *18*(2), 132-142.

[11] Hartl, F.U.; Hayer-Hartl, M. Protein folding - Molecular chaperones in the cytosol: from nascent chain to folded protein. *Science,* **2002**, *295*(5561), 1852-1858.

[12] Zietkiewicz, S.; Lewandowska, A.; Stocki, P.; Liberek, K. Hsp70 chaperone machine remodels protein aggregates at the initial step of Hsp70-Hsp100-dependent disaggregation. *J. Biol. Chem.,* **2006**, *281*(11), 7022-7029.

[13] Liberek, K.; Lewandowska, A.; Zietkiewicz, S. Chaperones in control of protein disaggregation. *EMBO J.,* **2008**, *27*(2), 328-335.

[14] Beissinger, M.; Buchner, J. How chaperones fold proteins. *Biol. Chem.,* **1998**, *379*(3), 245-259.

[15] Buchner, J. Hsp90 & Co. a holding for folding. *Trends Biochem. Sci.,* **1999**, *24*(4), 136-141.

[16] Gava, L.M.; Ramos, C.H.I. Human 90 kDa heat shock protein Hsp90 as a target for cancer therapeutics. *Curr. Chem. Biol.,* **2009**, *3*(1), 10-21.

[17] Seraphim, T.V.; Alves, M.M.; Silva, I.M.; Gomes, F.E.; Silva, K.P.; Murta, S.M.; Barbosa, L.R.; Borges, J.C. Low resolution structural studies indicate that the activator of Hsp90 ATPase 1 (Aha1) of Leishmania braziliensis has an elongated shape which allows its interaction with both N- and M-domains of Hsp90. *PLoS One,* **2013**, *8*(6), e66822.

[18] Silva, K.P.; Seraphim, T.V.; Borges, J.C. Structural and functional studies of Leishmania braziliensis Hsp90. *BBA - Proteins Proteom.,* **2013**, *1834*(1), 351-361.

[19] da Silva, V.C.; Ramos, C.H. The network interaction of the human cytosolic 90 kDa heat shock protein Hsp90: A target for cancer therapeutics. *J. Proteomics,* **2012**, *75*(10), 2790-2802.

[20] Pearl, L.H.; Prodromou, C. Structure and mechanism of the Hsp90 molecular chaperone machinery. *Annu. Rev. Biochem.,* **2006**, *75*, 271-294.

[21] Wandinger, S.K.; Richter, K.; Buchner, J. The Hsp90 chaperone machinery. *J. Biol. Chem.,* **2008**, *283*(27), 18473-18477.

[22] Mayer, M.P.; Bukau, B. Hsp70 chaperones: cellular functions and molecular mechanism. *Cell Mol. Life Sci.,* **2005**, *62*(6), 670-684.

[23] Seraphim, T.V.; Ramos, C.H.I.; Borges, J.C. *The interaction networks of Hsp70 and Hsp90 in the Plasmodium and Leishmania parasites. In: The Molecular Chaperones Interaction Networks in Protein Foldingand Degradation, Interactomics and Systems Biology*. 1 ed: New York, **2014**.

[24] Fan, A.C.Y.; Young, J.C. Function of Cytosolic Chaperones in Tom70-Mediated Mitochondrial Import. *Protein Pept. Lett.,* **2011**, *18*(2), 122-131.

[25] Ali, M.M.; Roe, S.M.; Vaughan, C.K.; Meyer, P.; Panaretou, B.; Piper, P.W.; Prodromou, C.; Pearl, L.H. Crystal structure of an Hsp90-nucleotide-p23/Sba1 closed chaperone complex. *Nature,* **2006**, *440*(7087), 1013-1017.

[26] Hessling, M.; Richter, K.; Buchner, J. Dissection of the ATP-induced conformational cycle of the molecular chaperone Hsp90. *Nat. Struct. Mol. Biol.,* **2009**, *16*(3), 287-293.

[27] Li, J.; Soroka, J.; Buchner, J. The Hsp90 chaperone machinery: conformational dynamics and regulation by co-chaperones. *Biochim Biophys Acta,* **2012**, *1823*(3), 624-635.

[28] Ratzke, C.; Berkemeier, F.; Hugel, T. Heat shock protein 90's mechanochemical cycle is dominated by thermal fluctuations. *Proc. Natl. Acad. Sci. U. S. A.,* **2012**, *109*(1), 161-166.

[29] Cano, L.Q.; Lavery, D.N.; Bevan, C.L. Mini-review: Foldosome regulation of androgen receptor action in prostate cancer. *Mol. Cell Endocrinol.,* **2013**, *369*(1-2), 52-62.

[30] Matts, R.L.; Dixit, A.; Peterson, L.B.; Sun, L.; Voruganti, S.; Kalyanaraman, P.; Hartson, S.D.; Verkhivker, G.M.; Blagg, B.S. Elucidation of the Hsp90 C-terminal inhibitor binding site. *ACS Chem. Biol.,* **2011**, *6*(8), 800-807.

[31] Bhat, R.; Tummalapalli, S.R.; Rotella, D.P. Progress in the Discovery and Development of Heat Shock Protein 90 (Hsp90) Inhibitors. *J. Med. Chem.,* **2014**, *57*(21), 8718-8728.

[32] Martínez-Alonso, M.; González-Montalbán, N.; García-Fruitós, E.; Villaverde, A. The Functional quality of soluble recombinant polypeptides produced in Escherichia coli is defined by a wide conformational spectrum. *Appl. Environ. Microbiol.,* **2008**, *74*(23), 7431-7433.

[33] Dimitrov, D.S. Therapeutic proteins. *Methods Mol. Biol.,* **2012**, *899*, 1-26.

[34] Manta, B.; Obal, G.; Ricciardi, A.; Pritsch, O.; Denicola, A. Tools to evaluate the conformation of protein products. *Biotechnol. J.,* **2011**, *6*(6), 731-741.

[35] García-Fruitós, E.; Vazquez, E.; Gonzalez-Montalbán, N.; Ferrer-Miralles, N.; Villaverde, A. Analytical approaches for assessing aggregation of protein biopharmaceuticals. *Curr. Pharm. Biotechnol.,* **2011**, *12*(10), 1530-1536.

[36] Bristow, A.F.; Bird, C.; Bolgiano, B.; Thorpe, R. Regulatory requirements for therapeutic proteins: the relationship between the conformation and biological activity of filgrastim. *Pharmeur. Bio. Sci. Notes,* **2012**, *2012*, 103-117.

[37] Falconer, R.J.; Collins, B.M. Survey of the year 2009: applications of isothermal titration calorimetry. *J. Mol. Recognit.,* **2011**, *24*(1), 1-16.

[38] Schreiber, G.; Keating, A.E. Protein binding specificity versus promiscuity. *Curr. Opin. Struct. Biol.,* **2011**, *21*(1), 50-61.

[39] Johnson, M.E.; Hummer, G. Nonspecific binding limits the number of proteins in a cell and shapes their interaction networks. *Proc. Natl. Acad. Sci. U. S. A.,* **2011**, *108*(2), 603-608.

[40] Mirzarezaee, M.; Araabi, B.N.; Sadeghi, M. Features analysis for identification of date and party hubs in protein interaction network of Saccharomyces Cerevisiae. *BMC Syst. Biol.,* **2010**, *4*, 172.

[41] Andorf, C.M.; Honavar, V.; Sen, T.Z. Predicting the binding patterns of hub proteins: a study using yeast protein interaction networks. *PLoS One,* **2013**, *8*(2), e56833.

[42] Taipale, M.; Jarosz, D.F.; Lindquist, S. HSP90 at the hub of protein homeostasis: emerging mechanistic insights. *Nat. Rev. Mol. Cell Biol.,* **2010**, *11*(7), 515-528.

[43] Wilkinson, K.D. *Quantitative Analysis of Protein–Protein Interactions In: Protein–Protein Interactions: Methods and Protocols*. Humana Press: Totowa, NJ, **2004**.

[44] Kastritis, P.L.; Bonvin, A.M. On the binding affinity of macromolecular interactions: daring to ask why proteins interact. *J. R. Soc. Interface,* **2013**, *10*(79), 20120835.

[45] Jelesarov, I.; Bosshard, H.R. Isothermal titration calorimetry and differential scanning calorimetry as complementary tools to investigate the energetics of biomolecular recognition. *J. Mol. Recognit.,* **1999**, *12*(1), 3-18.

[46] Chaires, J.B. Calorimetry and thermodynamics in drug design. *Annu. Rev. Biophys.,* **2008**, *37*, 135-151.

[47] Pierce, M.M.; Raman, C.S.; Nall, B.T. Isothermal titration calorimetry of protein-protein interactions. *Methods,* **1999**, *19*(2), 213-221.

[48] Wiseman, T.; Williston, S.; Brandts, J.F.; Lin, L.N. Rapid measurement of binding constants and heats of binding using a new titration calorimeter. *Anal. Biochem.,* **1989**, *179*(1), 131-137.

[49] Vuignier, K.; Schappler, J.; Veuthey, J.L.; Carrupt, P.A.; Martel, S. Drug-protein binding: a critical review of analytical tools. *Anal. Bioanal. Chem.,* **2010**, *398*(1), 53-66.

[50] Liang, Y. Applications of isothermal titration calorimetry in protein science. *Acta Biochim. Biophys. Sin. (Shanghai),* **2008**, *40*(7), 565-576.

[51] Lafont, V.; Armstrong, A.A.; Ohtaka, H.; Amzel, L.M.; Kiso, Y.; Freire, E. Enthalpy/Entropy compensation and the optimization of binding affinity. *Biophys. J.,* **2007**, *511*, (A).

[52] Ladbury, J.E. Calorimetry as a tool for understanding biomolecular interactions and an aid to drug design. *Biochem. Soc. Trans.,* **2010**, *38*(4), 888-893.

[53] Ferenczy, G.G.; Keserű, G.M. Thermodynamics guided lead discovery and optimization. *Drug Discov. Today,* **2010**, *15*(21-22), 919-932.

[54] Ladbury, J.E.; Klebe, G.; Freire, E. Adding calorimetric data to decision making in lead discovery: a hot tip. *Nat. Rev. Drug. Discov.,* **2010**, *9*(1), 23-27.

[55] Ohtaka, H.; Freire, E. Adaptive inhibitors of the HIV-1 protease. *Prog. Biophys. Mol. Biol.,* **2005**, *88*(2), 193-208.

[56] Freire, E.; Mayorga, O.L.; Straume, M. Isothermal Titration Calorimetry. *Anal. Chem.,* **1990**, *62*(18), A950-A959.

[57] Ladbury, J.E. Application of isothermal titration calorimetry in the biological sciences: things are heating up! *Biotechniques,* **2004**, *37*(6), 885-887.

[58] Baker, B.M.; Murphy, K.P. Prediction of binding energetics from structure using empirical parameterization. *Methods Enzymol.,* **1998**, *295*, 294-315.

[59] Todd, M.J.; Gomez, J. Enzyme kinetics determined using calorimetry: a general assay for enzyme activity? *Anal. Biochem.,* **2001**, *296*(2), 179-187.

[60] Bianconi, M.L. Calorimetric determination of thermodynamic parameters of reaction reveals different enthalpic compensations of the yeast hexokinase isozymes. *J. Biol. Chem.,* **2003**, *278*(21), 18709-18713.

[61] Hanlon, A.D.; Larkin, M.I.; Reddick, R.M. Free-Solution, Label-Free Protein-Protein Interactions Characterized by Dynamic Light Scattering. *Biophys. J.,* **2010**, *98*(2), 297-304.

[62] Kendrick, B.S.; Kerwin, B.A.; Chang, B.S.; Philo, J.S. Online Size-Exclusion High-Performance Liquid Chromatography Light Scattering and Differential Refractometry Methods to Determine Degree of Polymer Conjugation to Proteins and Protein–Protein or Protein–Ligand Association States. *Anal. Biochem.,* **2001**, *299*(2), 136-146.

[63] Lundblad, R.L. In *Protein Science Series*. Group, T.a.F., Ed.; Chapman & Hall/CRC: Boca Raton, FL, **2010**, pp 111-130.

[64] Wen, J.; Arakawa, T.; Philo, J.S. Size-exclusion chromatography with on-line light-scattering, absorbance, and refractive index detectors for studying proteins and their interactions. *Anal. Biochem.,* **1996**, *240*(2), 155-166.

[65] Striegel, A.; Yau, W.W.; Kirkland, J.J.; Bly, D.D. *Modern Size-Exclusion Liquid Chromatography: Practice of Gel Permeation and Gel Filtration Chromatography*. 2nd Edition ed. John Wiley & Sons Ed.: Hoboken, New Jersey, **2009**.

[66] Podzimek, S. *Light Scattering, Size Exclusion Chromatography and Asymmetric Flow Field Flow Fractionation: Powerful Tools for the Characterization of Polymers, Proteins and Nanoparticles*. John Wiley & Sons Ed.: Hoboken, New Jersey, **2011**.

[67] Hong, P.; Koza, S.; Bouvier, E.S.P. A review size-exclusion chromatography for the analysis of protein biotherapeutics and their aggregates. *J. Liq. Chromatogr. R. T.,* **2012**, *35*(20), 2923-2950.

[68] Bloomfield, V.A. In *On-Line Biophysics Textbook*. Schuster, T.M., Ed., **2000**; Vol. *Separations and Hydrodynamics*, pp 1-16.

[69] Some, D.; Kenrick, S. In *Protein Interactions*. Jianfeng, C.; Wang, R.E., Eds.; InTech: Rijeka, Croatia, **2012**, pp 401-426.

[70] Wyatt, P.J. Light scattering and the absolute characterization of macromolecules. *Anal. Chim. Acta,* **1993**, *272*(1), 1-40.

[71] Zölls, S.; Tantipolphan, R.; Wiggenhorn, M.; Winter, G.; Jiskoot, W.; Friess, W.; Hawe, A. Particles in therapeutic protein formulations, Part 1: Overview of analytical methods. *J. Pharm. Sci.,* **2012**, *101*(3), 914-935.

[72] Some, D. Light-scattering-based analysis of biomolecular interactions. *Biophys. Rev.,* **2013**, *5*(2), 147-158.

[73] Borges, J.C.; Ramos, C.H. Analysis of molecular targets of Mycobacterium tuberculosis by analytical ultracentrifugation. *Curr. Med. Chem.,* **2011**, *18*(9), 1276-1285.

[74] Lebowitz, J.; Lewis, M.S.; Schuck, P. Modern analytical ultracentrifugation in protein science: a tutorial review. *Protein Sci.,* **2002**, *11*(9), 2067-2079.

[75] Lamm, O. Die Differentialgleichung der Ultrazentrifugierung. *Ark. Mat. Astr. Fys.,* **1929**, *21*(B), 1-4.

[76] Berkowitz, S.A. Role of analytical ultracentrifugation in assessing the aggregation of protein biopharmaceuticals. *AAPS J.,* **2006**, *8*(3), E590-605.

[77] Howlett, G.J.; Minton, A.P.; Rivas, G. Analytical ultracentrifugation for the study of protein association and assembly. *Curr. Opin. Chem. Biol.,* **2006**, *10*(5), 430-436.

[78] Laue, T.M.; Stafford, W.F. Modern applications of analytical ultracentrifugation. *Annu. Rev. Biophys. Biomol. Struct.,* **1999**, *28*, 75-100.

[79] Lakowicz, J.R. *Principles of Fluorescence Spectroscopy*. Third ed. Springer: New York, **2006**.

[80] Albani, J.R. *STRUCTURE AND DYNAMICS OF MACROMOLECULES: ABSORPTION AND FLUORESCENCE STUDIES*. First ed. Elsevier Science, **2004**.

[81] Jameson, D.M.; Croney, J.C.; Moens, P.D. Fluorescence: basic concepts, practical aspects, and some anecdotes. *Methods Enzymol.,* **2003**, *360*, 1-43.

[82] Royer, C.A. Probing protein folding and conformational transitions with fluorescence. *Chem. Rev.,* **2006**, *106*(5), 1769-1784.

[83] Yan, Y.; Marriott, G. Analysis of protein interactions using fluorescence technologies. *Curr. Opin. Chem. Biol.,* **2003**, *7*(5), 635-640.

[84] Brown, M.P.; Royer, C. Fluorescence spectroscopy as a tool to investigate protein interactions. *Curr. Opin. Biotechnol.,* **1997**, *8*(1), 45-49.

[85] Weert, M.v.d.; Stella, L. Fluorescence quenching and ligand binding: A critical discussion of a popular methodology. *J. Mol. Struct.,* **2011**, *998*, 144-150.

[86] Mátyus, L.; Szöllosi, J.; Jenei, A. Steady-state fluorescence quenching applications for studying protein structure and dynamics. *J. Photochem. Photobiol. B,* **2006**, *83*(3), 223-236.

[87] Jablonski, A., Depolarization of Fluorescence of Liquid Solutions. *Bull. Acad. Polon. Sci., Ser. Sci. Math. Astr. Phys.,* **1960**, *8*, 655-660.

[88] Tetin, S.Y.; Hazlett, T.L. Optical spectroscopy in studies of antibody-hapten interactions. *Methods,* **2000**, *20*(3), 341-361.

[89] Pantoliano, M.W.; Petrella, E.C.; Kwasnoski, J.D.; Lobanov, V.S.; Myslik, J.; Graf, E.; Carver, T.; Asel, E.; Springer, B.A.; Lane, P.; Salemme, F.R. High-density miniaturized thermal shift assays as a general strategy for drug discovery. *J. Biomol. Screen.,* **2001**, *6*(6), 429-440.

[90] Boivin, S.; Kozak, S.; Meijers, R. Optimization of protein purification and characterization using Thermofluor screens. *Protein Expr. Purif.,* **2013**, *91*(2), 192-206.

[91] Vedadi, M.; Niesen, F.H.; Allali-Hassani, A.; Fedorov, O.Y.; Finerty, P.J.; Wasney, G.A.; Yeung, R.; Arrowsmith, C.; Ball, L.J.; Berglund, H.; Hui, R.; Marsden, B.D.; Nordlund, P.; Sundstrom, M.; Weigelt, J.; Edwards, A.M. Chemical screening methods to identify ligands that promote protein stability, protein crystallization, and structure determination. *PNAS,* **2006**, *103*(43), 15835-15840.

[92] Ericsson, U.B.; Hallberg, B.M.; DeTitta, G.T.; Dekker, N.; Nordlund, P. Thermofluor-based high-throughput stability optimization of proteins for structural studies. *Anal. Biochem.,* **2006**, *357*(2), 289-298.

[93] Tiroli-Cepeda, A.O.; Lima, T.B.; Balbuena, T.S.; Gozzo, F.C.; Ramos, C.H. Structural and functional characterization of the chaperone Hsp70 from sugarcane. Insights into conformational changes during cycling from cross-linking/mass spectrometry assays. *J. Proteomics,* **2014**, *104*, 48-56.

[94] Borges, J.C.; Ramos, C.H. Characterization of nucleotide-induced changes on the quaternary structure of human 70 kDa heat shock protein Hsp70.1 by analytical ultracentrifugation. *BMB Rep.,* **2009**, *42*(3), 166-171.

[95] Araujo, T.L.; Borges, J.C.; Ramos, C.H.; Meyer-Fernandes, J.R.; Oliveira Júnior, R.S.; Pascutti, P.G.; Foguel, D.; Palhano, F.L. Conformational changes in human Hsp70 induced by high hydrostatic pressure produce oligomers with ATPase activity but without chaperone activity. *Biochemistry,* **2014**, *53*(18), 2884-2889.

[96] Borges, J.C.; Ramos, C.H. Spectroscopic and thermodynamic measurements of nucleotide-induced changes in the human 70-kDa heat shock cognate protein. *Arch. Biochem. Biophys.,* **2006**, *452*(1), 46-54.

[97] Deocaris, C.C.; Kaul, S.C.; Wadhwa, R. In *Mortalin biology: life, stress and death*. Kaul, S.C.; Wadhwa, R., Eds.; Dordrecht: Springer, c2012.: New York, **2012**, pp 21-30.

[98] Lu, W.J.; Lee, N.P.; Kaul, S.C.; Lan, F.; Poon, R.T.P.; Wadhwa, R.; Luk, J.M. Mortalin-p53 interaction in cancer cells is stress dependent and constitutes a selective target for cancer therapy. *Cell Death Differ.,* **2011**, *18*(6), 1046-1056.

[99] Kaul, S.C.; Deocaris, C.C.; Wadhwa, R. Three faces of mortalin: A housekeeper, guardian and killer. *Exp.Gerontol.,* **2007**, *42*(4), 263-274.

[100] Dores-Silva, P.R.; Barbosa, L.R.S.; Ramos, C.H.I.; Borges, J.C. Human Mitochondrial Hsp70 (Mortalin): Shedding Light on ATPase Activity, Interaction with Adenosine Nucleotides, Solution Structure and Domain Organization. *PLoS One,* **2015**, *10*(1), e0117170.

[101] Montgomery, D.L.; Morimoto, R.I.; Gierasch, L.M. Mutations in the substrate binding domain of the Escherichia coli 70 kDa molecular chaperone, DnaK, which alter substrate affinity or interdomain coupling. *J. Mol. Biol.,* **1999**, *286*(3), 915-932.

[102] Kundrat, L.; Regan, L. Balance between folding and degradation for Hsp90-dependent client proteins: a key role for CHIP. *Biochemistry,* **2010**, *49*(35), 7428-7438.

[103] Dores-Silva, P.R.; Silva, E.R.; Gomes, F.E.; Silva, K.P.; Barbosa, L.R.; Borges, J.C. Low resolution structural characterization of the Hsp70-interacting protein - Hip - from Leishmania braziliensis emphasizes its high asymmetry. *Arch. Biochem. Biophys.,* **2012**, *520*(2), 88-98.

[104] Hohfeld, J.; Minami, Y.; Hartl, F.U. Hip, A Novel Cochaperone Involved in the Eukaryotic Hsc70/Hsp40 Reaction Cycle. *Cell,* **1995**, *83*(4), 589-598.

[105] Silva, J.C.; Borges, J.C.; Cyr, D.M.; Ramos, C.H.I.; Torriani, I.L. Central domain deletions affect the SAXS solution structure and function of Yeast Hsp40 proteins Sis1 and Ydj1. *BMC Struct. Biol.,* **2011**, *11*, 40.

[106] Ramos, C.H.I.; Oliveira, C.L.P.; Fan, C.Y.; Torriani, I.L.; Cyr, D.M. Conserved Central Domains Control the Quaternary Structure of Type I and Type II Hsp40 Molecular Chaperones. *J. Mol. Biol.,* **2008**, *383*(1), 155-166.

[107] Borges, J.; Fischer, H.; Craievich, A.F.; Ramos, C.H. Low resolution structural study of two human HSP40 chaperones in solution - DjA1 from subfamily A and DjB4 from subfamily B have different quaternary structures. *J. Biol. Chem.,* **2005**, *280*(14), 13671-13681.

[108] Summers, D.W.; Douglas, P.M.; Ramos, C.H.I.; Cyr, D.M. Polypeptide transfer from Hsp40 to Hsp70 molecular chaperones. *Trends Biochem.Sci.,* **2009**, *34*(5), 230-233.

[109] Borges, J.C.; Seraphim, T.V.; Mokry, D.Z.; Almeida, F.C.L.; Cyr, D.M.; Ramos, C.H.I. Identification of Regions Involved in Substrate Binding and Dimer Stabilization within the Central Domains of Yeast Hsp40 Sis1. *Plos One,* **2012**, *7*(12), e50927.

[110] Sichting, M.; Mokranjac, D.; Azem, A.; Neupert, W.; Hell, K. Maintenance of structure and function of mitochondrial Hsp70 chaperones requires the chaperone Hep1. *EMBO J.,* **2005**, *24*(5), 1046-1056.

[111] Dores-Silva, P.R.; Minari, K.; Ramos, C.H.I.; Barbosa, L.R.S.; Borges, J.C. Structural and stability studies of the human mtHsp70-escort protein 1: An essential mortalin co-chaperone. *Int. J. Biol. Macromol.,* **2013**, *56*, 140-148.

[112] Rousaki, A.; Miyata, Y.; Jinwal, U.K.; Dickey, C.A.; Gestwicki, J.E.; Zuiderweg, E.R. Allosteric drugs: the interaction of antitumor compound MKT-077 with human Hsp70 chaperones. *J. Mol. Biol.,* **2011**, *411*(3), 614-632.

[113] Chang, L.; Miyata, Y.; Ung, P.M.; Bertelsen, E.B.; McQuade, T.J.; Carlson, H.A.; Zuiderweg, E.R.; Gestwicki, J.E. Chemical screens against a reconstituted multiprotein complex: myricetin blocks DnaJ regulation of DnaK through an allosteric mechanism. *Chem. Biol.,* **2011**, *18*(2), 210-221.

[114] Hainzl, O.; Lapina, M.C.; Buchner, J.; Richter, K. The charged linker region is an important regulator of Hsp90 function. *J. Biol. Chem.,* **2009**, *284*(34), 22559-22567.

[115] Mendonça, Y.A.; Ramos, C.H. Cloning, purification and characterization of a 90kDa heat shock protein from Citrus sinensis (sweet orange). *Plant Physiol. Biochem.,* **2012**, *50*(1), 87-94.

[116] da Silva, V.C.; Cagliari, T.C.; Lima, T.B.; Gozzo, F.C.; Ramos, C.H. Conformational and functional studies of a cytosolic 90 kDa heat shock protein Hsp90 from sugarcane. *Plant Physiol. Biochem.,* **2013**, *68*, 16-22.

[117] McLaughlin, S.H.; Ventouras, L.A.; Lobbezoo, B.; Jackson, S.E. Independent ATPase activity of Hsp90 subunits creates a flexible assembly platform. *J. Mol. Biol.,* **2004**, *344*(3), 813-826.

[118] Nilapwar, S.; Williams, E.; Fu, C.; Prodromou, C.; Pearl, L.H.; Williams, M.A.; Ladbury, J.E. Structural-thermodynamic relationships of interactions in the N-terminal ATP-binding domain of Hsp90. *J. Mol. Biol.,* **2009**, *392*(4), 923-936.

[119] Fan, A.C.; Gava, L.M.; Ramos, C.H.; Young, J.C. Human mitochondrial import receptor Tom70 functions as a monomer. *BioChem. J.,* **2010**, *429*(3), 553-563.

[120] Gava, L.M.; Goncalves, D.C.; Borges, J.C.; Ramos, C.H.I. Stoichiometry and thermodynamics of the interaction between the C-terminus of human 90 kDa heat shock protein Hsp90 and the mitochondrial translocase of outer membrane Tom70. *Arch. Biochem. Biophys.,* **2011**, *513*(2), 119-125.

[121] Onuoha, S.C.; Couistock, E.T.; Grossmann, J.G.; Jackson, S.E. Structural studies on the co-chaperone hop and its complexes with Hsp90. *J. Mol. Biol.,* **2008**, *379*(4), 732-744.

[122] McLaughlin, S.H.; Sobott, F.; Yao, Z.P.; Zhang, W.; Nielsen, P.R.; Grossmann, J.G.; Laue, E.D.; Robinson, C.V.; Jackson, S.E. The co-chaperone p23 arrests the Hsp90 ATPase cycle to trap client proteins. *J. Mol. Biol.,* **2006**, *356*(3), 746-758.

[123] Karagöz, G.E.; Duarte, A.M.; Ippel, H.; Uetrecht, C.; Sinnige, T.; van Rosmalen, M.; Hausmann, J.; Heck, A.J.; Boelens, R.; Rüdiger, S.G. N-terminal domain of human Hsp90 triggers binding to the cochaperone p23. *Proc. Natl. Acad. Sci. U. S. A.,* **2011**, *108*(2), 580-585.

[124] Siligardi, G.; Hu, B.; Panaretou, B.; Piper, P.W.; Pearl, L.H.; Prodromou, C. Co-chaperone regulation of conformational switching in the Hsp90 ATPase cycle. *J. Biol. Chem.,* **2004**, *279*(50), 51989-51998.

[125] Batista, F.A.H.; Almeida, G.S.; Seraphim, T.V.; Silva, K.P.; Murta, S.M.F.; Barbosa, L.R.S.; Borges, J.C. Identification of two p23 co-chaperone isoforms in *Leishmania braziliensis* which exhibit similar structures and Hsp90 interaction properties despite divergent stabilities. *FEBS J.,* **2015**, *282*(2), 388-406.

[126] Paul, S.; Mahanta, S. Association of heat-shock proteins in various neurodegenerative disorders: is it a master key to open the therapeutic door? *Mol. Cell Biochem.,* **2014**, *386*(1-2), 45-61.

[127] Garcia-Carbonero, R.; Carnero, A.; Paz-Ares, L., Inhibition of HSP90 molecular chaperones: moving into the clinic. *Lancet Oncol.,* **2013**, *14*(9), e358-369.

[128] Calderwood, S.K. Molecular cochaperones: tumor growth and cancer treatment. *Scientifica (Cairo),* **2013**, *2013*, 217513.

[129] Taldone, T.; Patel, P.D.; Patel, M.; Patel, H.J.; Evans, C.E.; Rodina, A.; Ochiana, S.; Shah, S.K.; Uddin, M.; Gewirth, D.; Chiosis, G. Experimental and structural testing module to analyze paralogue-specificity and affinity in the Hsp90 inhibitors series. *J. Med. Chem.,* **2013**, *56*(17), 6803-6818.

[130] Pizarro, J.C.; Hills, T.; Senisterra, G.; Wernimont, A.K.; Mackenzie, C.; Norcross, N.R.; Ferguson, M.A.; Wyatt, P.G.; Gilbert, I.H.; Hui, R. Exploring the Trypanosoma brucei Hsp83 potential as a target for structure guided drug design. *PLoS Negl. Trop. Dis.,* **2013**, *7*(10), e2492.

[131] Kazlauskas, E.; Petrikaitė, V.; Michailovienė, V.; Revuckienė, J.; Matulienė, J.; Grinius, L.; Matulis, D. Thermodynamics of aryldihydroxyphenyl-thiadiazole binding to human Hsp90. *PLoS One,* **2012**, *7*(5), e36899.

[132] Debnath, A.; Shahinas, D.; Bryant, C.; Hirata, K.; Miyamoto, Y.; Hwang, G.; Gut, J.; Renslo, A.R.; Pillai, D.R.; Eckmann, L.; Reed, S.L.; McKerrow, J.H. Hsp90 inhibitors as new leads to target parasitic diarrheal diseases. *Antimicrob. Agents Chemother.,* **2014**, *58*(7), 4138-4144.

[133] Salminen, A.; Lehtonen, M.; Paimela, T.; Kaarniranta, K. Celastrol: Molecular targets of Thunder God Vine. *Biochem. Biophys. Res. Commun.,* **2010**, *394*(3), 439-442.

[134] Zanphorlin, L.M.; Alves, F.R.; Ramos, C.H. The effect of celastrol, a triterpene with antitumorigenic activity, on conformational and functional aspects of the human 90kDa heat shock protein Hsp90α, a chaperone implicated in the stabilization of the tumor phenotype. *Biochim. Biophys. Acta,* **2014**, *1840*(10), 3145-3152.

[135] Alexander, L.D.; Partridge, J.R.; Agard, D.A.; McAlpine, S.R. A small molecule that preferentially binds the closed conformation of Hsp90. *Bioorg. Med. Chem. Lett.,* **2011**, *21*(23), 7068-7071.

Received: October 13, 2014 Revised: October 29, 2014 Accepted: November 12, 2014